NASA Contractor Report 165888

NASA-CR-165888
19830010476

An Assessment of the Performance of the Spanwise Iron Magnet Rolling Moment Generating System for Magnetic Suspension and Balance Systems, Using the Finite Element Computer Program "GFUN"

C. P. Britcher

Department of Aeronautics and Astronautics
University of Southampton
England

Contract NSG-7523
April 1982

National Aeronautics and Space Administration

Langley Research Center
Hampton, Virginia 23665

AN ASSESSMENT OF THE PERFORMANCE OF THE SPANWISE IRON MAGNET ROLLING MOMENT GENERATING SYSTEM FOR MAGNETIC SUSPENSION AND BALANCE SYSTEMS, USING THE FINITE ELEMENT COMPUTER PROGRAM "GFUN"

by

C.P. BRITCHER

Department of Aeronautics and Astronautics
University of Southampton
England.

January 1982

This report covers work undertaken on NASA Grant NSG-7523, entitled "Investigations into the Technology Required to Raise Reliability Levels of Magnetic Suspension". The Principal Investigator is Dr. M.J. Goodyer and the NASA Technical Officer is Mr. R.P. Boyden of NASA Langley Research Center.

CONTENTS

SYMBOLS AND ABBREVIATIONS

AR	Wing aspect ratio
E/M	Electromagnet
J	Current density (in Amperes/cm^2)
J_r	Current density in E/Ms generating through wing field
J_m	Current density in E/Ms generating spanwise magnetizing field
$J_{r,m}$	J_r and J_m as above
LMSBS	Large Magnetic Suspension and Balance System
M	Induced magnetization defined from: $B = M + \mu_o H$ where B and M expressed in Tesla and H in A/m. This formulation for M is not to SI standard but avoids use of symbol J for polarization.
SIM	Spanwise Iron Magnet
t/c	Wing thickness to chord ratio
μ	Relative permeability

Disclaimer

The use of trade names in this report in no way implies any endorsment of product or manufacturer.

1. INTRODUCTION

A key difficulty to be overcome before construction of a Large Magnetic Suspension and Balance System (LMSBS) could be undertaken is identification of a system of rolling moment generation with adequate torque capability. To date, no D.C. System had been shown to be sufficiently powerful and the existing A.C. System (1), whilst potentially capable of high torques, seems unsuited to LMSBS application due to the requirement for high amplitude A.C. applied fields. This report presents some preliminary computed data concerning a relatively new D.C. scheme for rolling moment generation, referred to as the Spanwise Iron Magnet (SIM) scheme (2).

1.1. The principle of rolling moment generation by Spanwise Iron Magnets

Symmetrically disposed transverse magnetization components can relatively easily be induced in a magnetically soft wing core by application of a symmetrical field as shown below:

Fig.1 SIM magnetizing field.

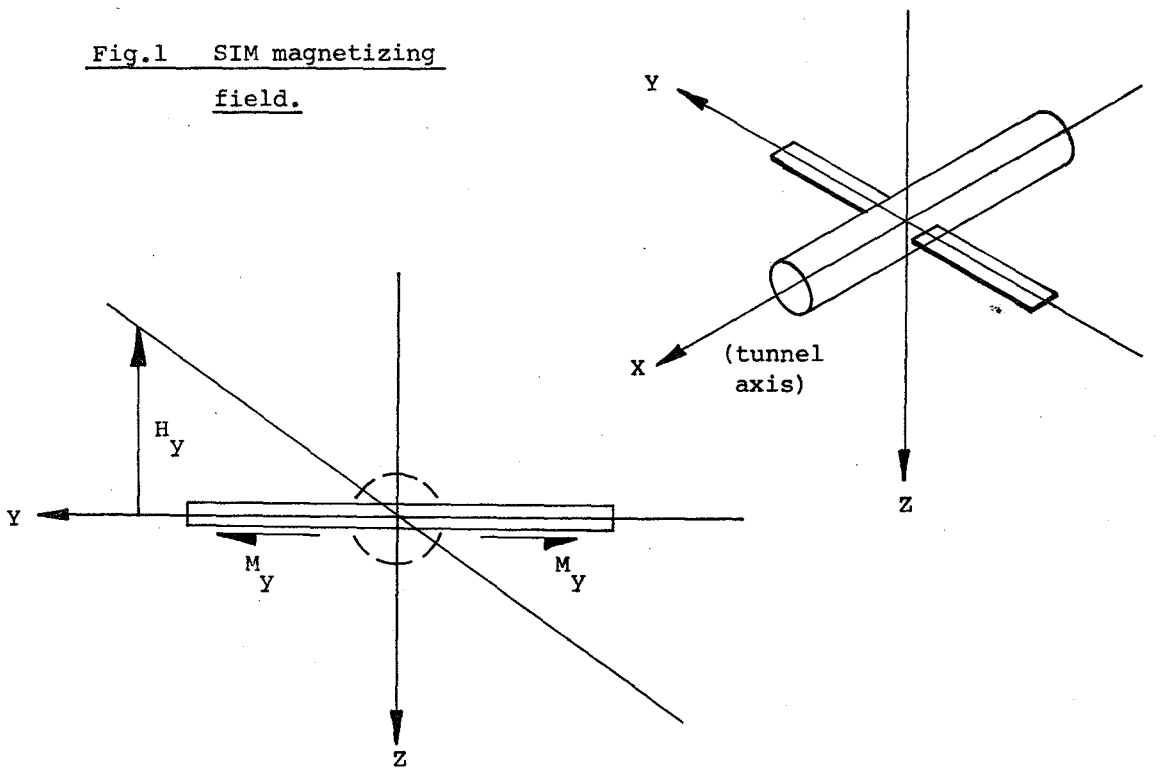

This type of field can be produced elegantly by a classical dipole:

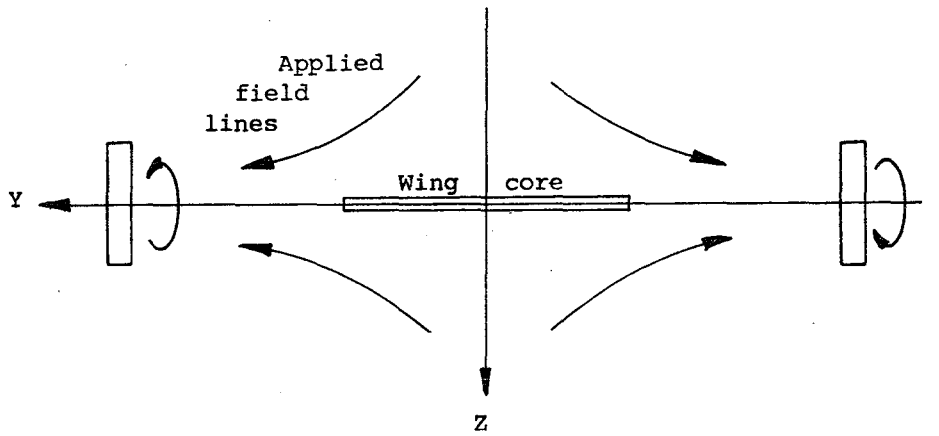

Fig.2 SIM dipole magnetizing field.

or quadrupole field:

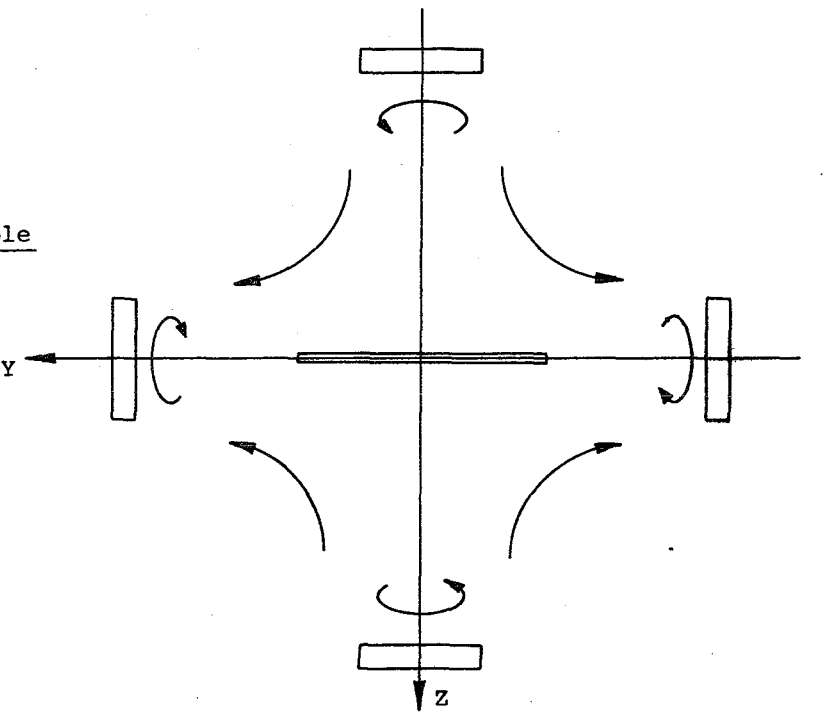

Fig.3 SIM quadrupole magnetizing field

Rolling moment will be generated with application of through wing fields as in Figure 4. Rotation of the induced spanwise magnetization vectors by the through wing fields will be inhibited by the high demagnetizing factors in the through-wing direction. Calculation of the performance of SIM systems is not straight forward, the induced magnetizations not being directly analytic.

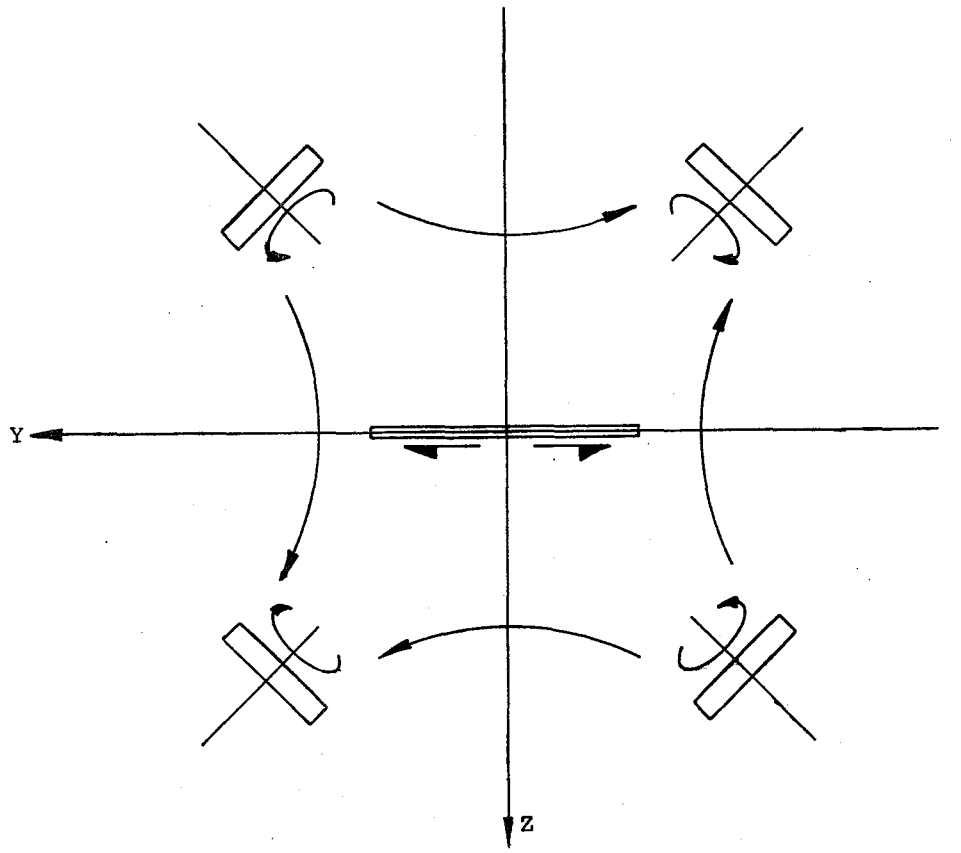

Fig.4 SIM "roll" field.

2. SOLUTION OF IRON-AIR-CONDUCTOR MAGNETOSTATIC SYSTEMS

This class of problem has attracted considerable interest over recent years with the application of superconductors to various fields such as nuclear research and with the drive to improve performance and efficiency of electrical machines.

General magnetostatic problems involve the solution of Poisson's equation or, outside current carrying conductors, Laplace's equation. These equations may be solved in principle by a number of methods including (after (3))

1) Analogue 2) Graphical 3) Analytic 4) Numerical

Predictions of roll torque from SIMs requires treatment of saturation effects, leading to non-linear solutions, and are inherently three dimensional. In most practial cases methods 1) and 2) above are not able to handle the non-linear problem, indeed graphical methods are generally restricted to two dimensions. Analytic methods are available for non-linear 3D problems but only for highly restricted geometries of conductor and iron. Application to general

problems is currently quite impractical. Again following (3) existing numerical methods in this field may be divided into four principal catagories

1) Finite difference
2) Images
3) Integral equations
4) Variational formulations

although other classes of solution do exist, such as the Monte-Carlo method (4).

It would appear that image methods are **inapplicable** to non-linear problems within the bounds of the present formulations. Method (4) above may be considered an energy method, somewhat analogous to virtual work methods in structural problems, whereas 1) above tackles Poisson's or Laplace's equation directly but both generally require that the complete volume of the problem is meshed with a computation grid. The characteristic geometry of the SIM roll system is very "open", (Figure 5) that is a small iron region separated from the conductors by large air gaps. Methods 1) and 4) above would thus require meshing of considerable volumes of air, at least enclosing all the conductors, leading to large computation times. Integral equation methods (3 above) need only require meshing of iron regions and thus appear appropriate here.

2.1. Program GFUN

This program, developed at the Rutherford Laboratory, Didcot, Oxon, U.K. since 1970 by Trowbridge et al, is an example of the use of integral equation methods. GFUN has been applied to a wide range of problems over many years (3,5,6,7,8) and has exhibited consistently good accuracy, consequently gaining a high international reputation. A disadvantage inherent to the solution procedures employed is a somewhat awkward representation of field within iron regions, as the vector sum of the fields from external currents and induced magnetizations, expressed as constant within suitably shaped elements (such as tetrahedra). In high permeability regions the two contributions to the field may be nearly equal and opposite, leading to rather poor resolution of the internal field. GFUN in fact handles the simultaneous integral equations as a single matrix equation, solution of the latter generating eigen solutions for the internal field. Clearly prediction of the detail geometry of the internal field is affected by the choice of element distributions. The lack of precise information concerning the internal field of the SIM cores is not thought to be especially critical. It must be

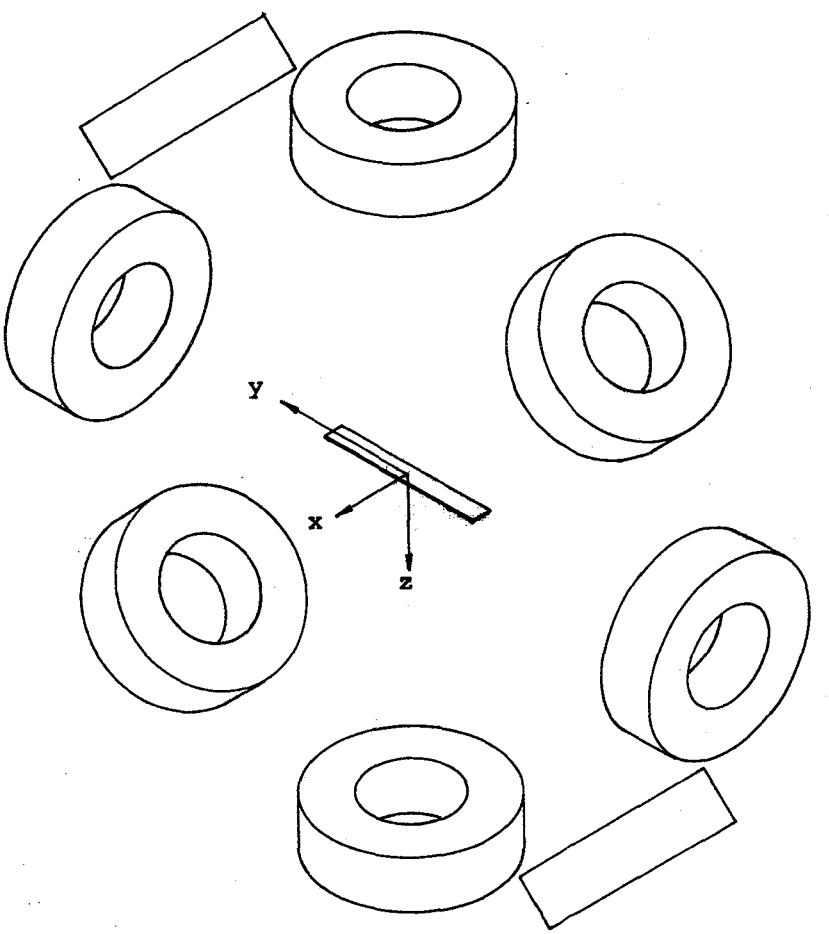

Fig.5 Characteristic configuration of SIM rolling moment generating system. (8 symmetrically disposed E/Ms)

noted that the nature of the solution procedure implies that the foregoing adverse comments do not apply outside the iron region, however paradoxical that may seem, and need not apply to the resolution of forces and torques provided methods of field integration over control volumes external to the iron are chosen.

Access to GFUN was granted by the British Science Research Council* under Grant No. GR/B/3691.5. Modifications to the program were carried out by Simkin to permit the full symmetry existing in many of the required SIM cases to be exploited (reducing computation time) and to provide a torque integration option. The torque integration scheme is conceptually similar to the well established methods for force calculations but the fact that previous users have apparently not required torque information must be seen to represent a major possible source of systematic error in data included hereafter, indeed some difficulties were experienced before a consistent integration scheme could be identified. To counter this uncertainty, various low field torque measurements have been made and limited cross checking undertaken (Section 4). Saturation of iron regions, which could not be acheived in corroborative experiments, should not directly influence the reliability of torque predictions due to the nature of the methods used.

2.2. Baseline GFUN geometry and configuration

A baseline geometry and configuration is required from which the effects of variations of various parameters, such as wing aspect ratio, may be examined. At the time of commencement of this study there existed no clear specific choice of geometry of either model or E/Ms, necessitating evolution of a baseline geometry on the following somewhat arbitrary basis.

The favoured scale for studies of LMSBSs has been for a test section of approximately 8 ft x 8 ft cross section (such as NTF). Calculations are therefore made at this scale, but the scaling of results to different tunnel sizes is quite straightforward (Appendix 1). The test section is assumed square with no corner fillets. Clearance is allowed around the aerodynamic cross section for structure, plenum chamber etc., and is chosen to be one foot (9). A similar allowance is made for the thermal insulation and structure surrounding each E/M (9). The most uncertain characteristics of the E/Ms are the winding shape and maximum useable

*Now the Science and Engineering Research Council.

current density. It appears (9) that manufacturers prefer circular windings where possible due to reduction of difficulties associated with conductor stressing. An idealized 8 E/M configuration has been chosen (Figure 6). The problem of optimizing the E/M array must be dealt with seperately, being heavily influenced by particular requirements for forces and moments in other degrees of freedom. Maximum useable overall current density (J) for superconducting E/Ms varies from order 1500 A/cm^2 for cryostable conductors to order 15000 A/cm^2 for adiabatically stable conductors, within the limits of present technology. Doubts exist (9) as to whether adiabatically stable conductors could be applied to the 8 ft scale case so generous winding cross sections are allowed in the E/Ms permitting partial saturation of the wing cores at suitably low values of J. High J data is included for the purpose of identifying trends at high field levels. The current levels in the E/Ms are represented by J_R and J_M as defined by Figure 6.

The geometry of the baseline SIM wing core is simply chosen as a 10% t/c, 10:1 AR rectangular hexahedron (rectangular "slab" core) spanning slightly under one half (49.2%) of the test section width, (Figure 7).

The choice of core material (or its magnetic characteristics) presents some difficulty at this stage due to the necessity in a final design to acheive an optimum compromise between many magnetic, electrical and mechanical properties. The SIM wing cores are visualized as occupying nearly all the aerodynamic volume of the wings with only those detail fittings and features potentially subject to changes during test programs being added from non-magnetic material. It is recognised that this view may require qualification in the light of detailed results, and experience in model design but it is nonetheless clear that the core material requires good mechanical properties such as high yield point, low brittleness and high Youngs Modulus, perhaps also at low temperatures. High electrical resistivity may be preferred in order to suppress eddy current flow in the cores but is not essential to fundamental operation of the system. Low coercive force is necessary to avoid torque calibration being dependent on the recent past magnetic history of the cores, although if cores are operated far into saturation this feature becomes of lesser importance. Ultra high permeability is not necessary since in any airgap dominated system iron regions of medium and higher permeabilities tend to behave as if infinitely permeable. The key magnetic parameter is undoubtedly saturation induction. Studies of LMSBSs (9) have indicated that valuable economies can be made in E/M size, hence cost,

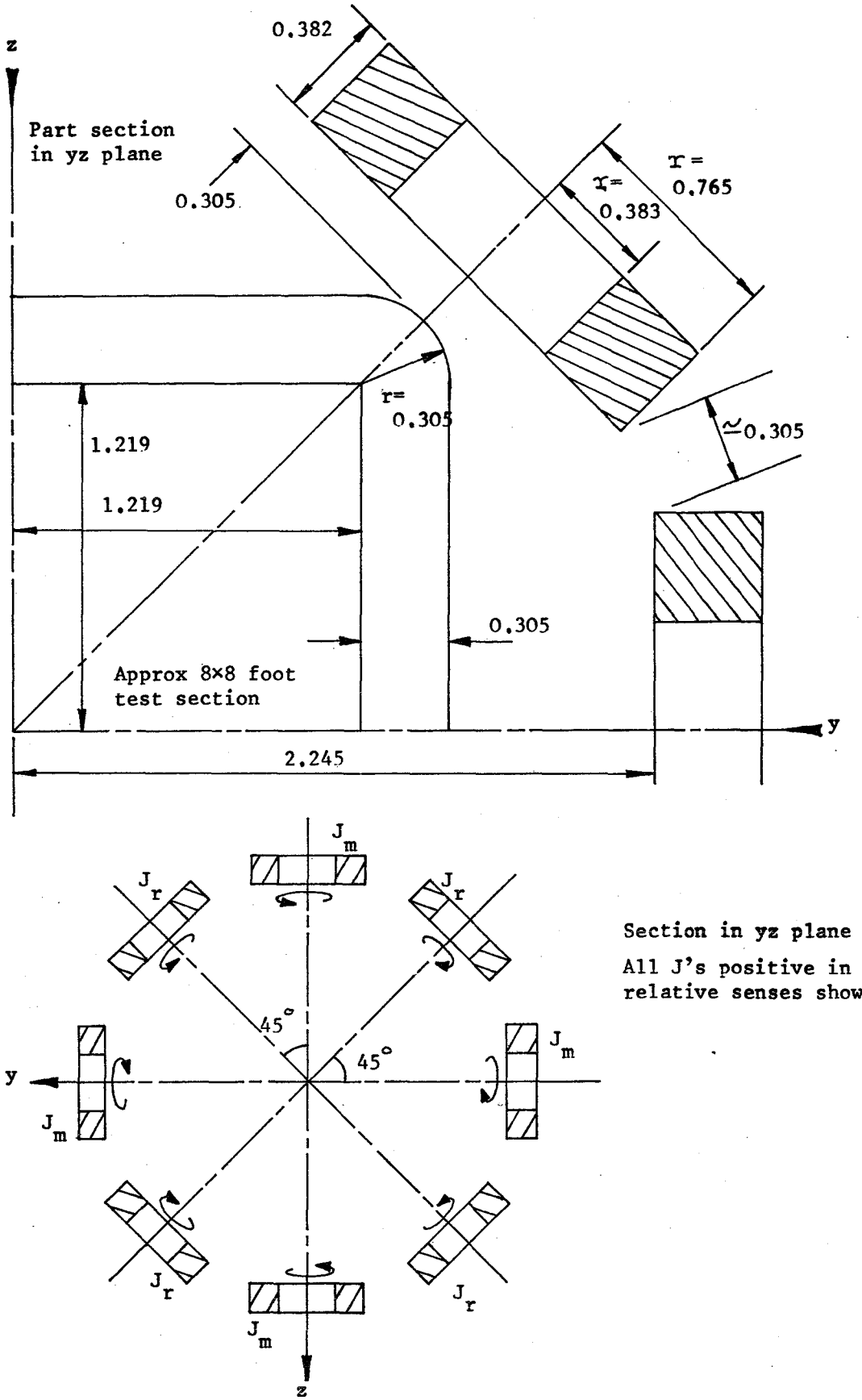

Fig.6 Baseline GFUN E/M geometry and configuration. Dims. in metres.

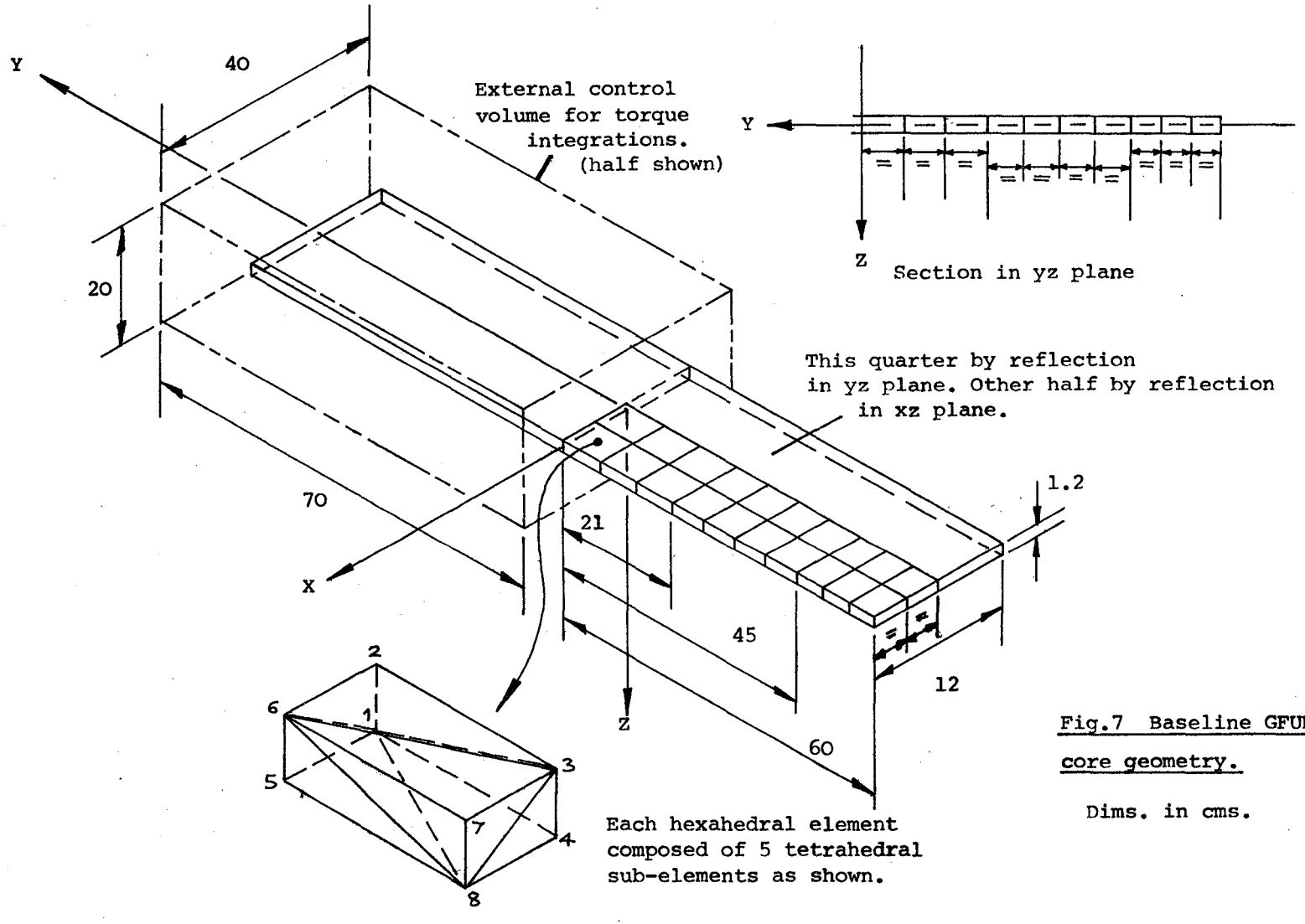

Fig.7 Baseline GFUN core geometry.

Dims. in cms.

(10)

by utilising fuselage core materials with the highest available saturation induction. It is logical that similar criteria should apply to the SIM case since operation of the core beyond the saturation point is anticipated.

One class of materials that appears promising is the cobalt iron alloys, classically represented by the 50:50 Fe:Co alloy "Permendur". These materials have not found widespread industrial application due to their relatively high cost but this is unlikely to be a problem in LMSBS application. Indeed the cost of a model core for an 8 ft tunnel has been estimated at U.S. $5000 (1981 $, Reference 9). This is small compared to a typical manufacturing cost of a large wind tunnel model.

Magnetic and mechanical properties of material of this type are dependent on the precise alloying constituents, heat treatment and preparation of samples but typical properties for some commercially available materials are shown below.

Material (Trade Name)	Permendur	Vanadium Permendur	Vacoflux 50
Source	Western Electric Co. Ltd.		Vacuumschmelze
Ref.	10	10	11
Density (g/cm^3)	8.3	8.3	8.15
Initial μ	800	800	1000
Saturation Induction (T)	2.45	2.4	2.35
Static coercivity (A/m)	159	159	110
Resistivity Ωm	0.7×10^{-6}	0.26×10^{-6}	0.35×10^{-6}
Youngs Modulus GPa	—	—	230
Yield strength MPa	—	—	400

It should be noted that the saturation inductions, in the range 2.35 - 2.45T (exceeding 2.5T in laboratory specimens) are substantially higher than the corresponding value for high purity iron of some 2.158T (room temperature, Ref 10).

The peaks in the permeability versus magnetizing field strength curves for the above materials (Figure 8) present some problems to GFUN. The permeability of each iron element in GFUN is assumed constant throughout the element and is updated at each iteration. Sharp rises in the permeability of elements with relatively small increases in the magnetizing field acting on those elements (and vice versa) occuring from one iteration to the next may cause local oscillations of the iron's interior field and consequently slow convergence. These potential problems may be avoided in early work by choosing a permeability versus magnetizing field strength characteristic that falls monotonically. This has been done by arbitrarily fitting intermediate points between the initial constant permeability line and the terminal saturation boundary, thus establishing the baseline characteristic shown in Figure 9. A slightly conservative value of 2.3T is chosen for M_{SAT}. The effects of variations of some material properties on the torque capability of the SIM system is studied later.

The baseline wing element distributions is chosen along well established principles. Tetrahedral elements have proven to be the most reliable choice for GFUN, the total number of elements is the largest that can be handled by the convenient batch version of the program and the spatial distribution of the elements is chosen such that the elements are relatively numerous in the region of strongest anticipated magnetization. This non-uniform element distribution also yields superior convergence. The control volume for use with the torque integration schemes is dimensioned such that its surfaces lie close to the model core, thus yielding best accuracy.

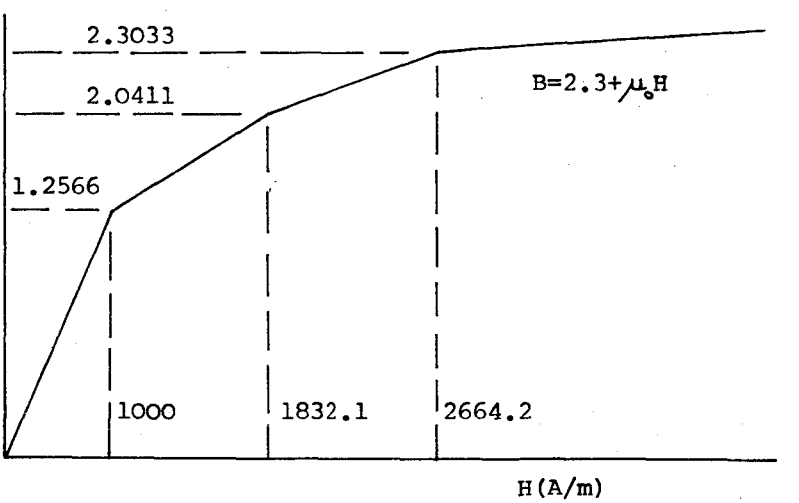

Fig.9 GFUN baseline permeability curve.

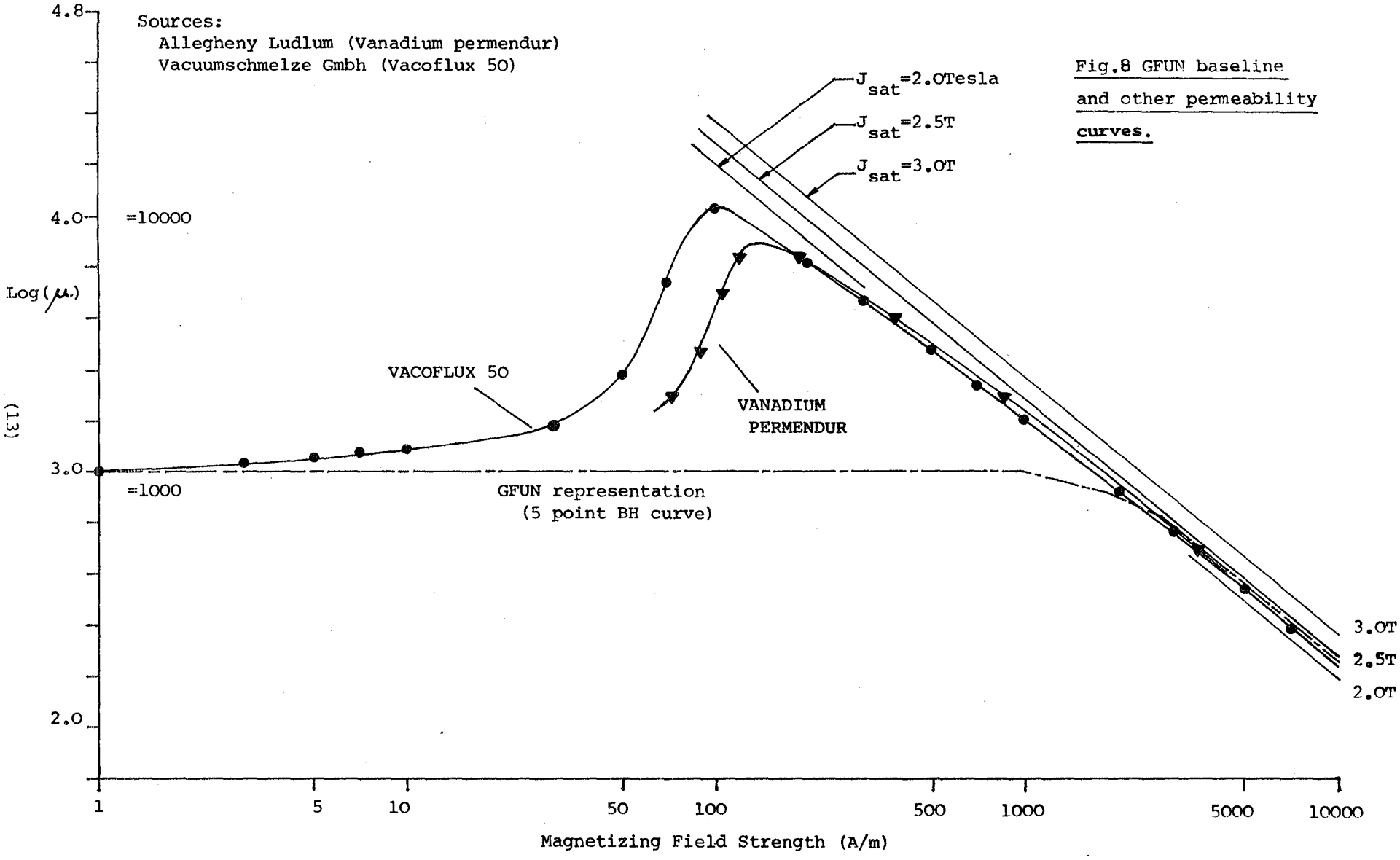

Fig.8 GFUN baseline and other permeability curves.

3. GFUN RESULTS

3.1. Baseline geometry - Effect of variation in material properties, low and intermediate applied fields

Where the permeability of the core is constant (linear solution, typical of low applied field levels) the effects of the magnetizing (J_M) and through-wing (J_R) fields are independant. Since, under these conditions, the spanwise magnetization is everywhere proportional to J_M and the through-wing field proportional to J_R the roll torque is expected to vary as the product $J_M J_R$. This is confirmed in Figures 10, 11, 12.

The variation of torque with core permeability, permeability held constant within each solution, is of interest, Figure 13 showing comparatively low sensitivity to permeability variations at high values of permeability, the core behaving as if infinitely permeable.

Using the baseline BH curve it is clear that there exists some maximum level of applied field commensurate with the whole core lying in the initial constant permeability region of the BH curve. At higher applied field levels the permeability of certain strongly magnetized volumes of the core will progressively fall, eventually the bulk of the core settling onto the terminal (saturated) region of the BH curve. During this process the magnetization is no longer proportional to J_M, rather reaching some limiting value. It might therefore be expected that torque becomes proportional to J_R alone. However at high values of through-wing field the induced magnetizations may no longer be predominantly spanwise, rather turning to lie more nearly parallel with the direction of local (applied) field. Torque may therefore reach some limiting value, or continue to rise (or fall) with rising applied fields as some function of J_R and J_M (Figure 14).

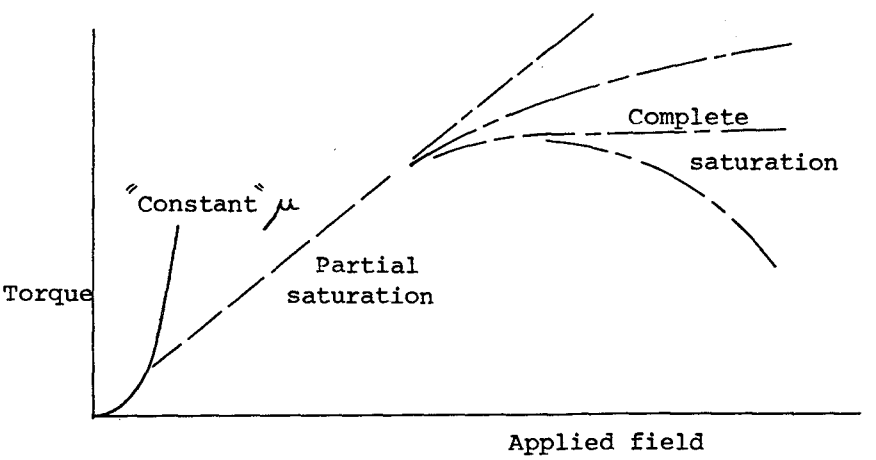

Fig.14 Schematic diagram showing possible terminal torque characteristics.

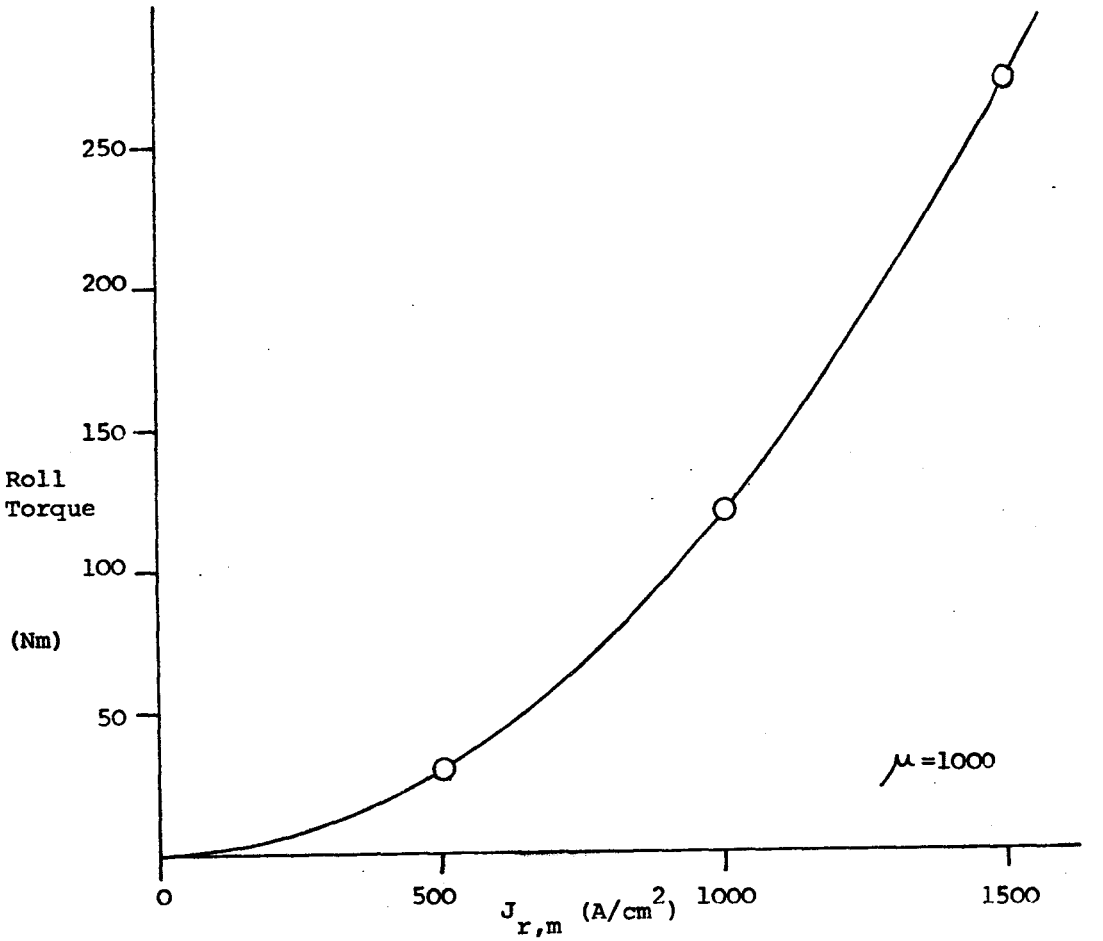

Fig.10 Torque versus $J_{r,m}$. Baseline core and E/Ms. Linear solutions.

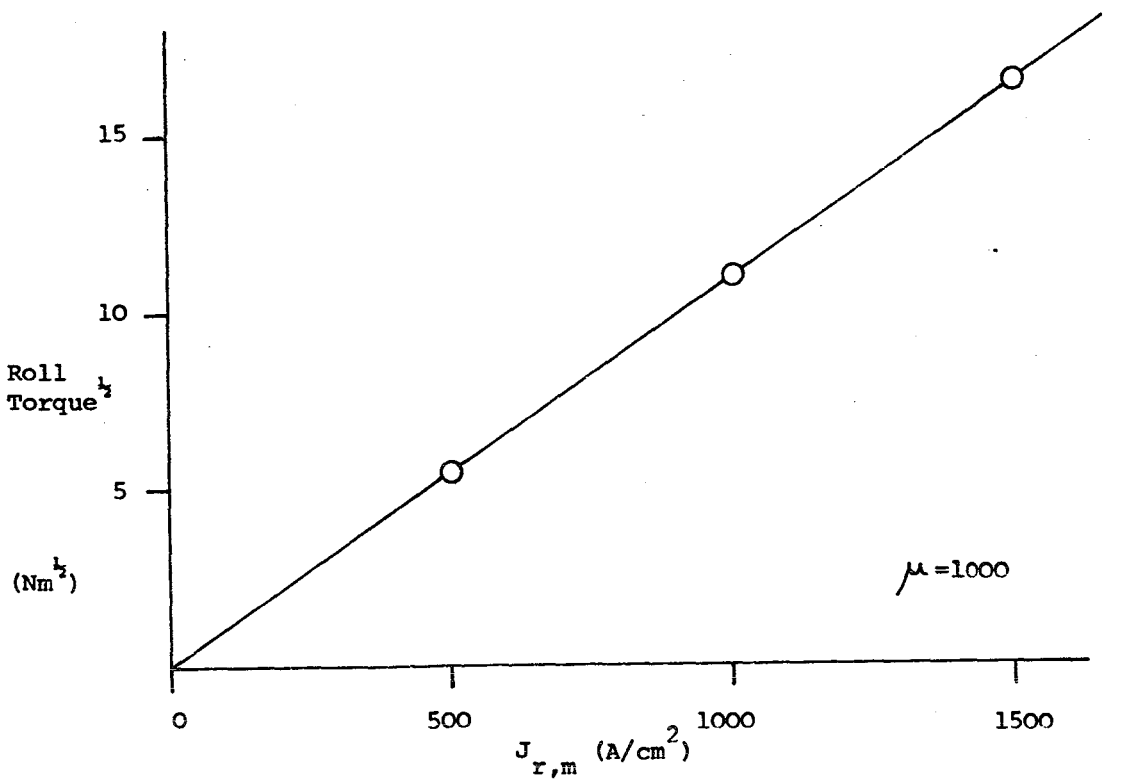

Fig.11 Root torque versus $J_{r,m}$. As Fig.10

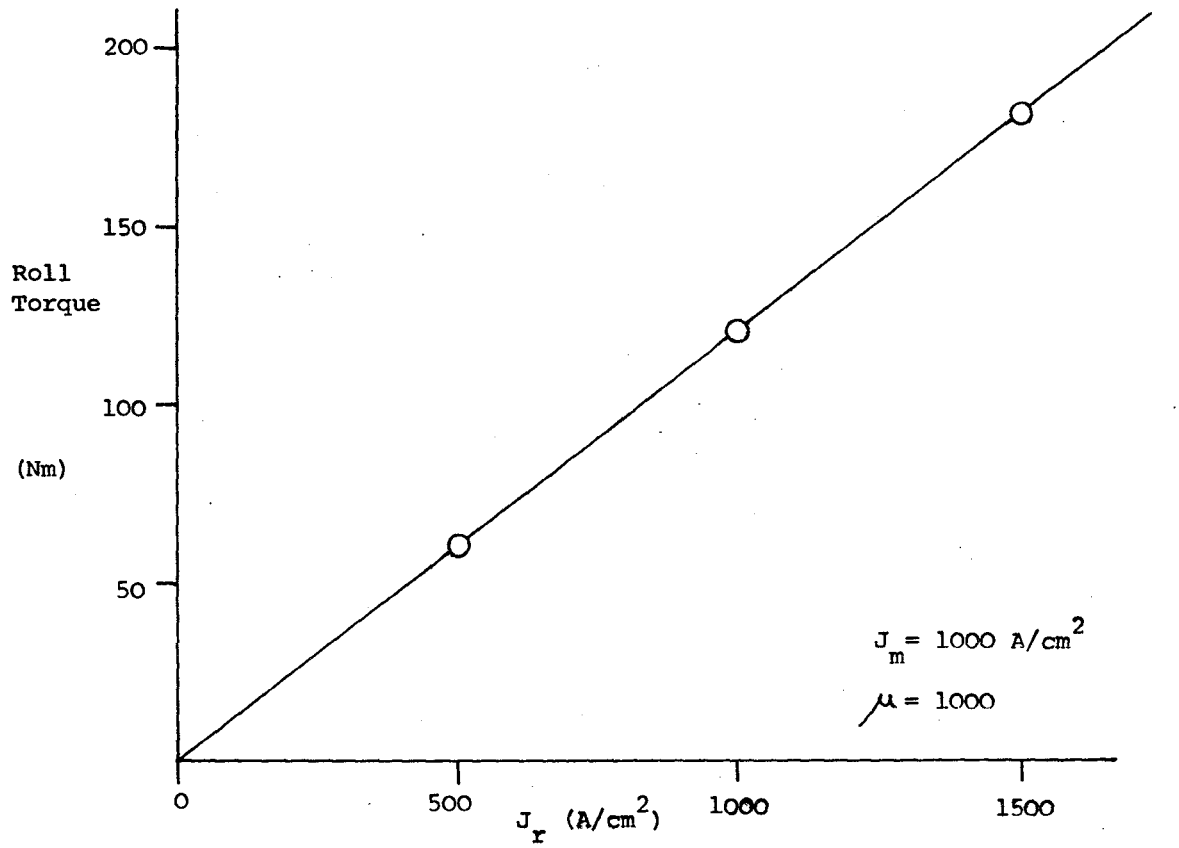

Fig.12 Torque versus J_r, J_m constant. Baseline core and E/Ms. Linear solutions.

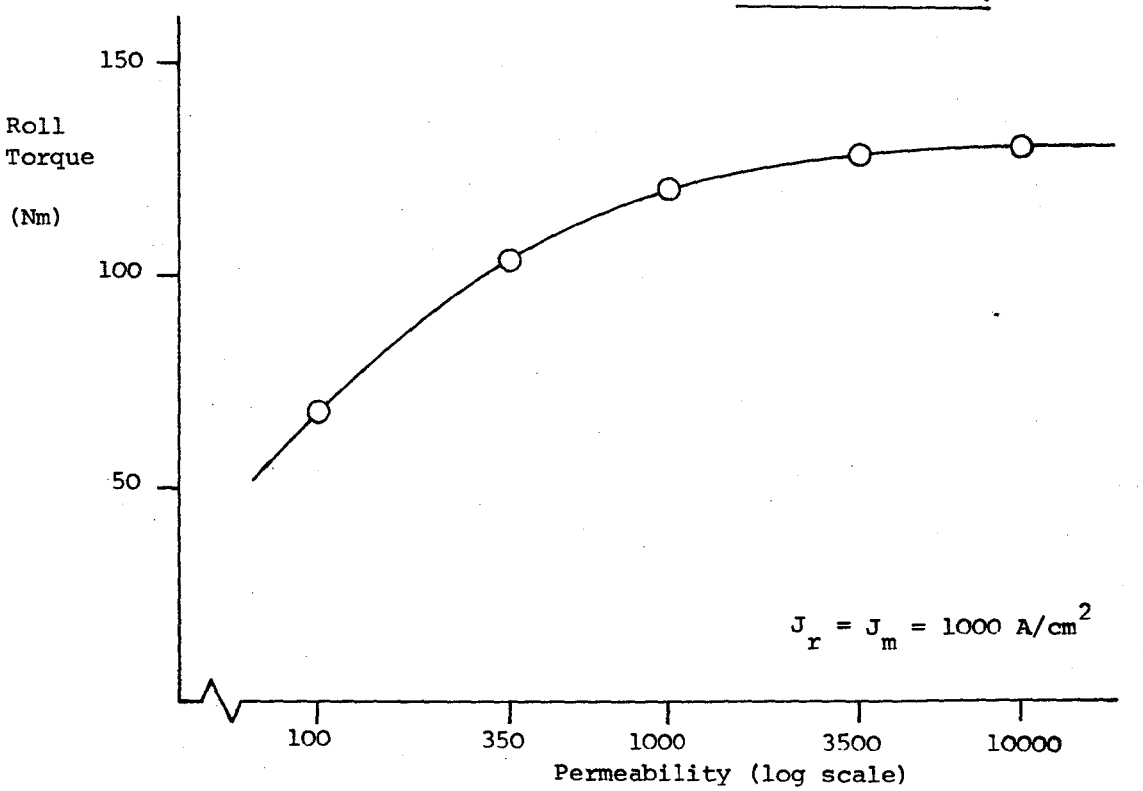

Fig.13 Torque versus permeability. Baseline core and E/Ms. Linear solutions.

Figures 15, 16 show the breakaway from the linear permeability curve onto a near straight line characteristic at moderate applied field levels. Data is included for a close approximation to the representative BH curve in Figure 9, showing a very weak influence of precise core magnetic properties.

3.2. Variations of baseline geometry. Effect of wing AR, t/c and taper

GFUN solves linear (constant permeability) cases directly, without recourse to iterative procedures, hence relatively economically. The variations of the initial (constant permeability) torque capability of the system with various geometrical parameters as defined in Figure 17 are shown in Figures 18, 19, 20, the solid symbols representing the baseline core.

These figures require some explanation. It is clear that the torque for a given applied field is far from being a constant per unit core volume and in fact does not obey any simple relation to geometry (such as first moment of volume about the x axis). It is believed that this effect is due to the fact that the effective spanwise demagnetizing factors are predominately determined by the slenderness of the core, being lower for more slender cases. Thus the removal of wing volume by reduction of chord or thickness lowers the effective spanwise demagnetizing factor, hence increasing the level of spanwise magnetization of the core for any given applied field level. This may be partly justified by inspection of Figures 21, 22 showing the increase in the peak element spanwise magnetization with increasing slenderness.

Tapering the core under the criteria chosen does not affect the core volume but displaces volume from the most effective regions near the tips to less effective regions near the roots. The slenderness of the tip portions of the core is increased and since these lie in the regions of strongest applied fields the peak value of element magnetization tends to be increased as shown in Figure 23.

3.3. Effect of the presence of fuselage and axial magnetizing field

It is to be expected that the presence of an unsaturated iron fuselage should act to increase the mean level of spanwise magnetization in the wing cores since it provides an easy flux path at the wing root (Figure 24). A saturated

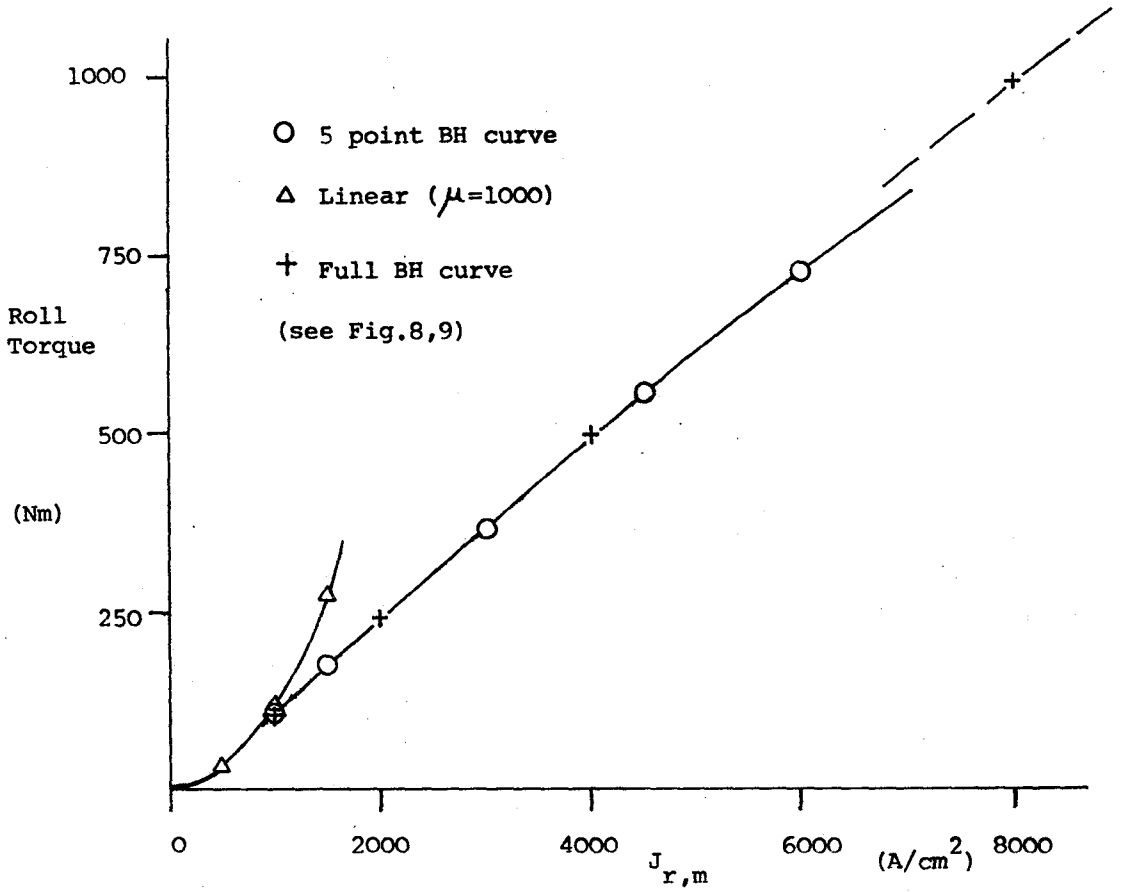

Fig.15 Torque versus $J_{r,m}$. Baseline core geometry and E/Ms

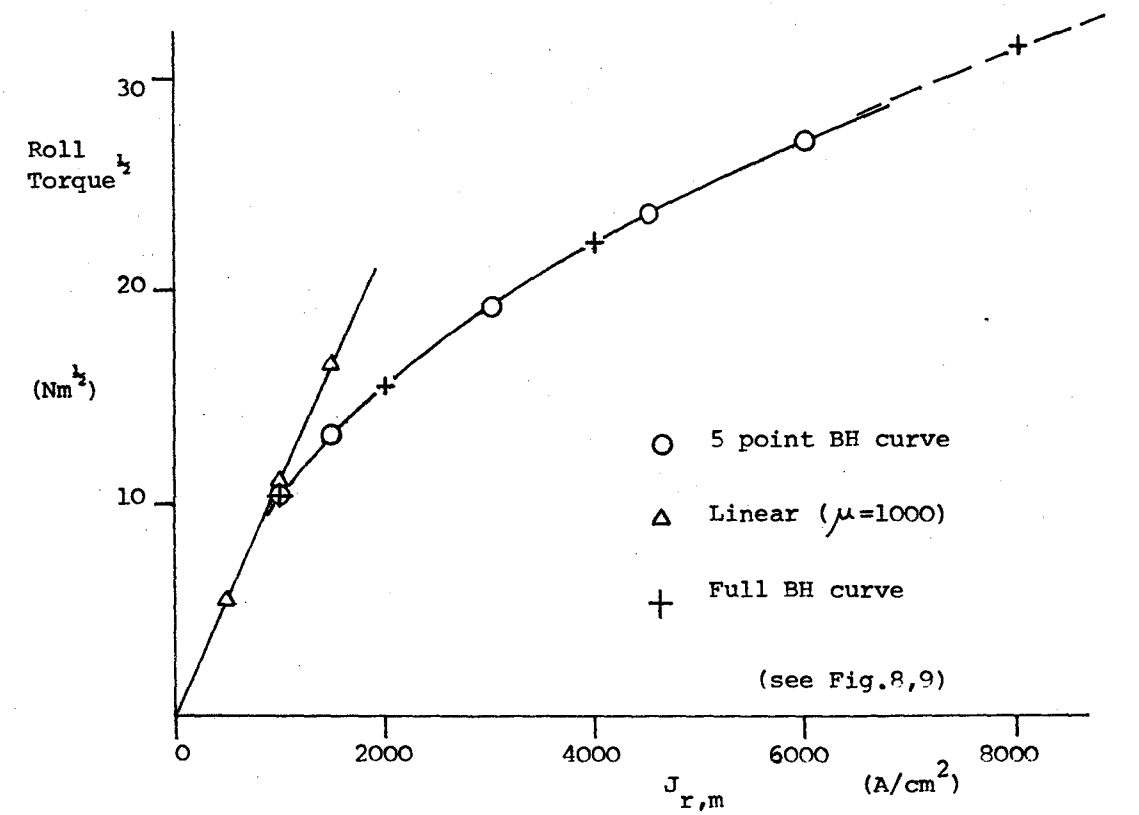

Fig.16 Root torque versus $J_{r,m}$. As Fig.15

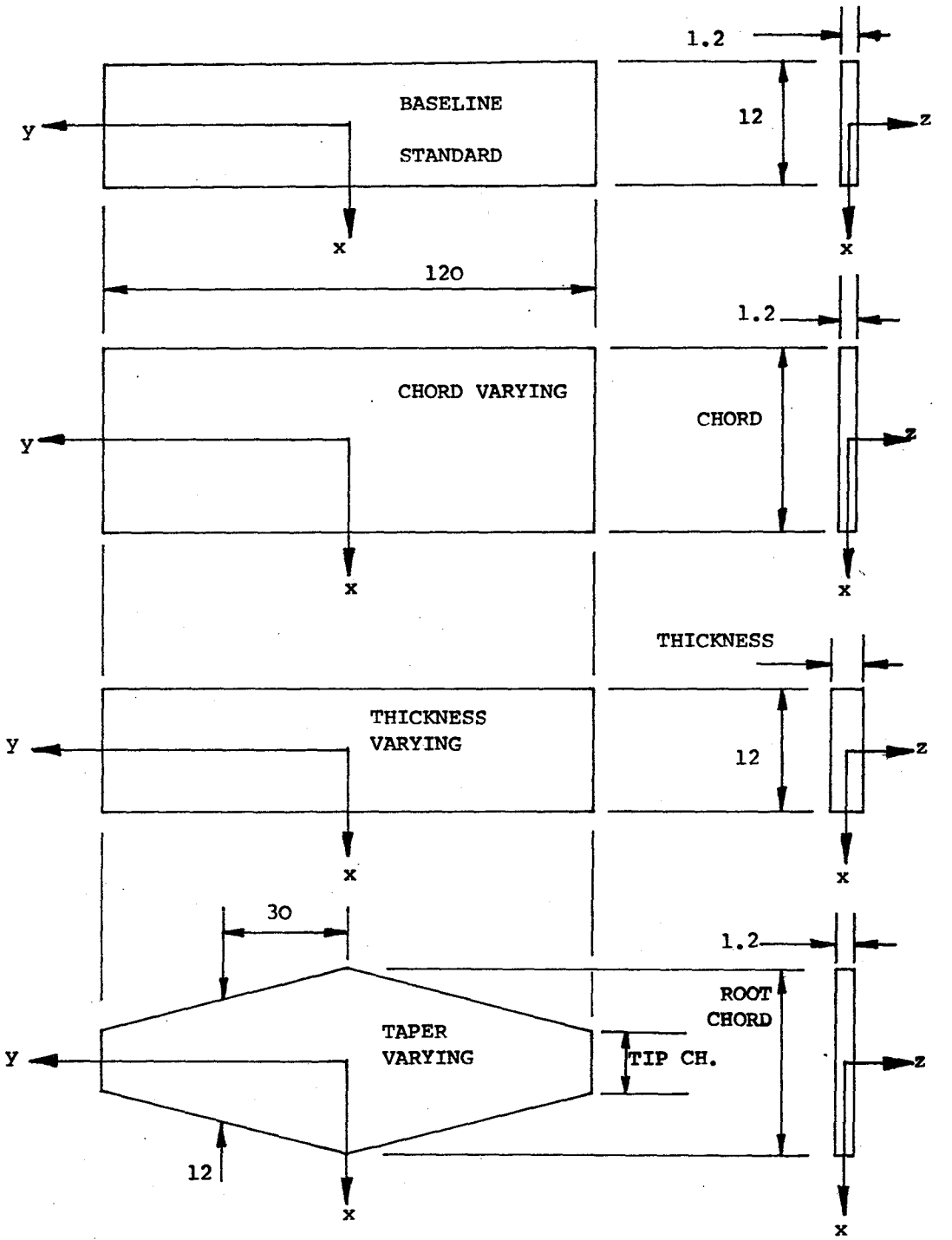

Fig. 17 Definitions of variations of baseline geometry.
all dimensions in cms.

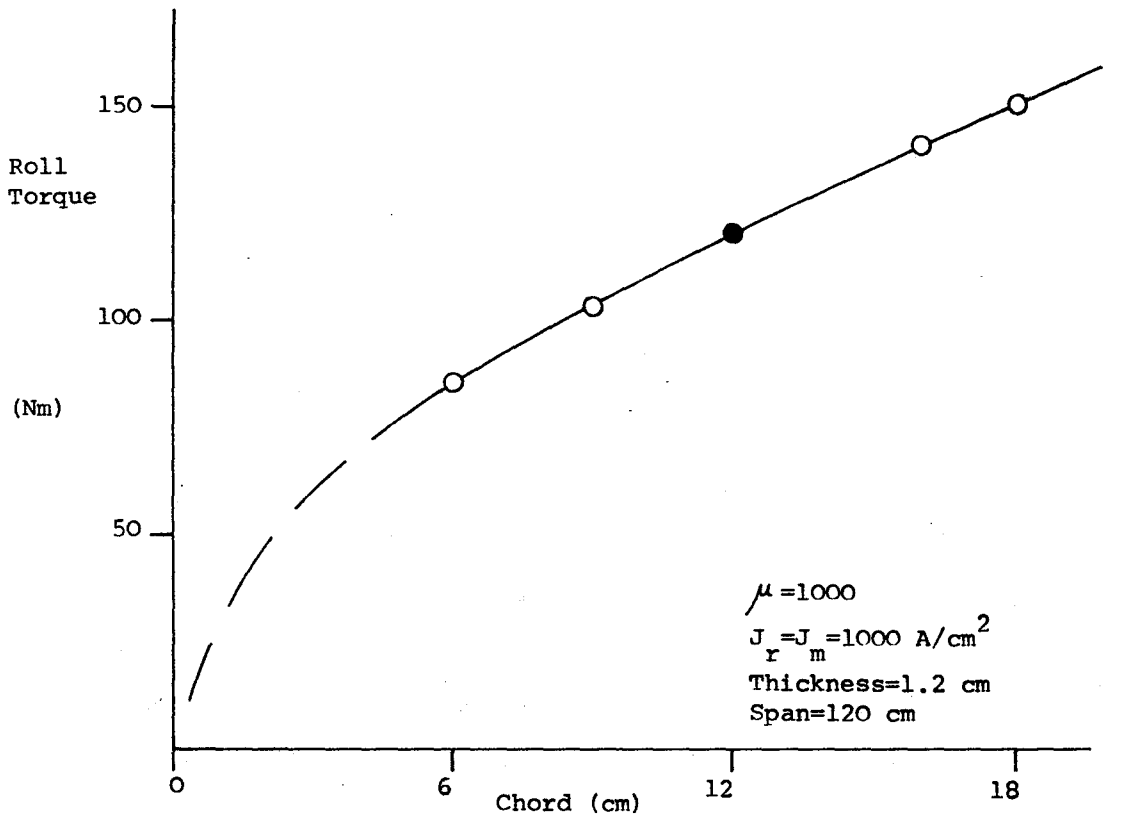

Fig.18 Torque versus chord. Baseline E/Ms. Core as Fig.17. Linear solutions.

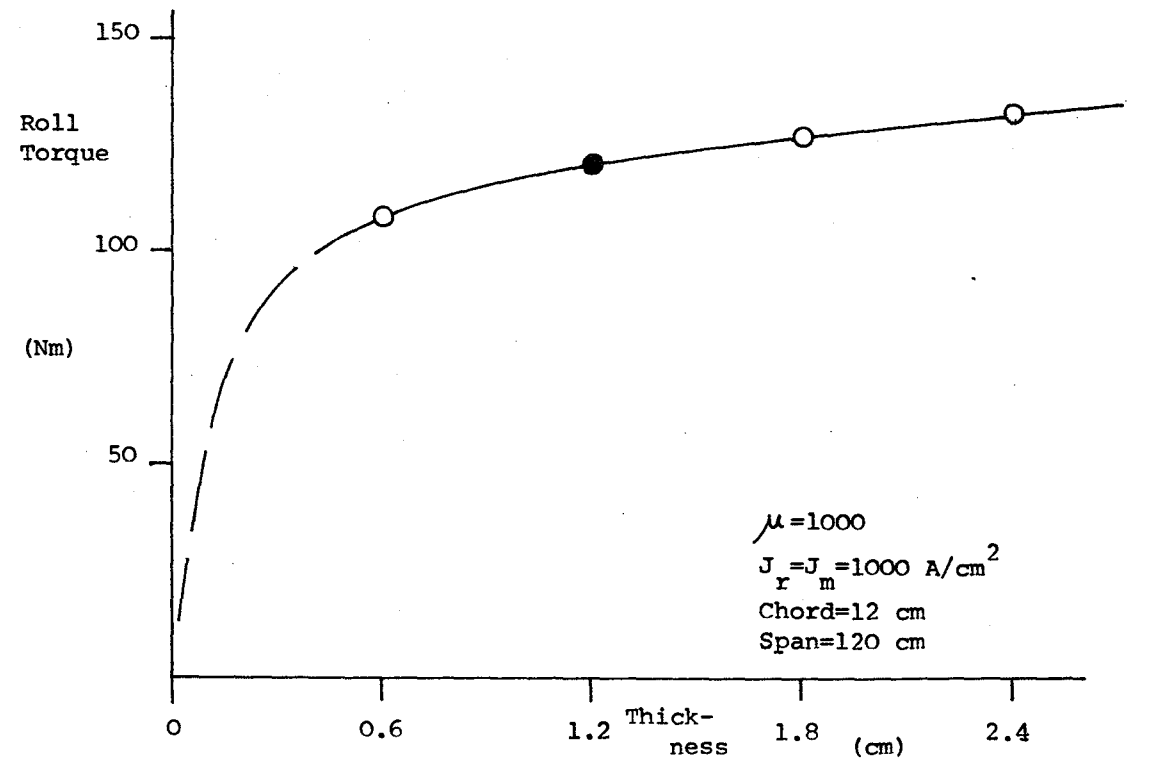

Fig.19 Torque versus thickness. Baseline E/Ms. Core as Fig.17 Linear solutions.

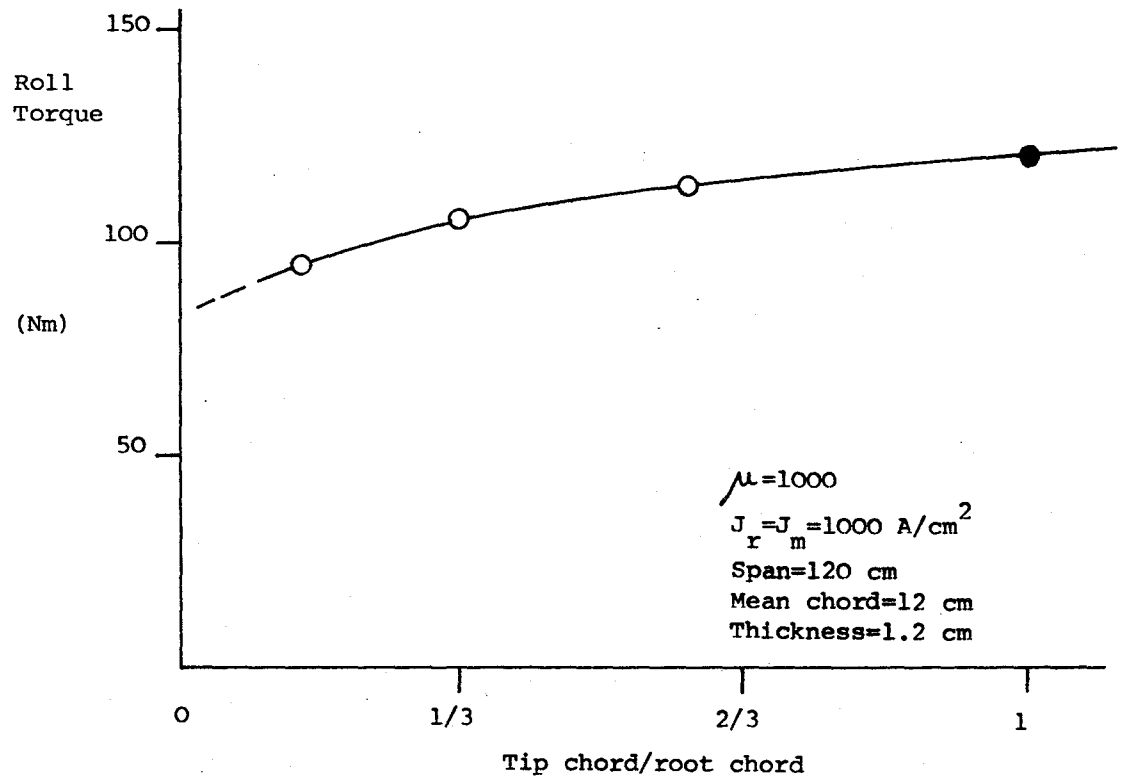

Fig.20 Torque versus taper. Baseline E/Ms. Core as Fig.17. Linear solutions.

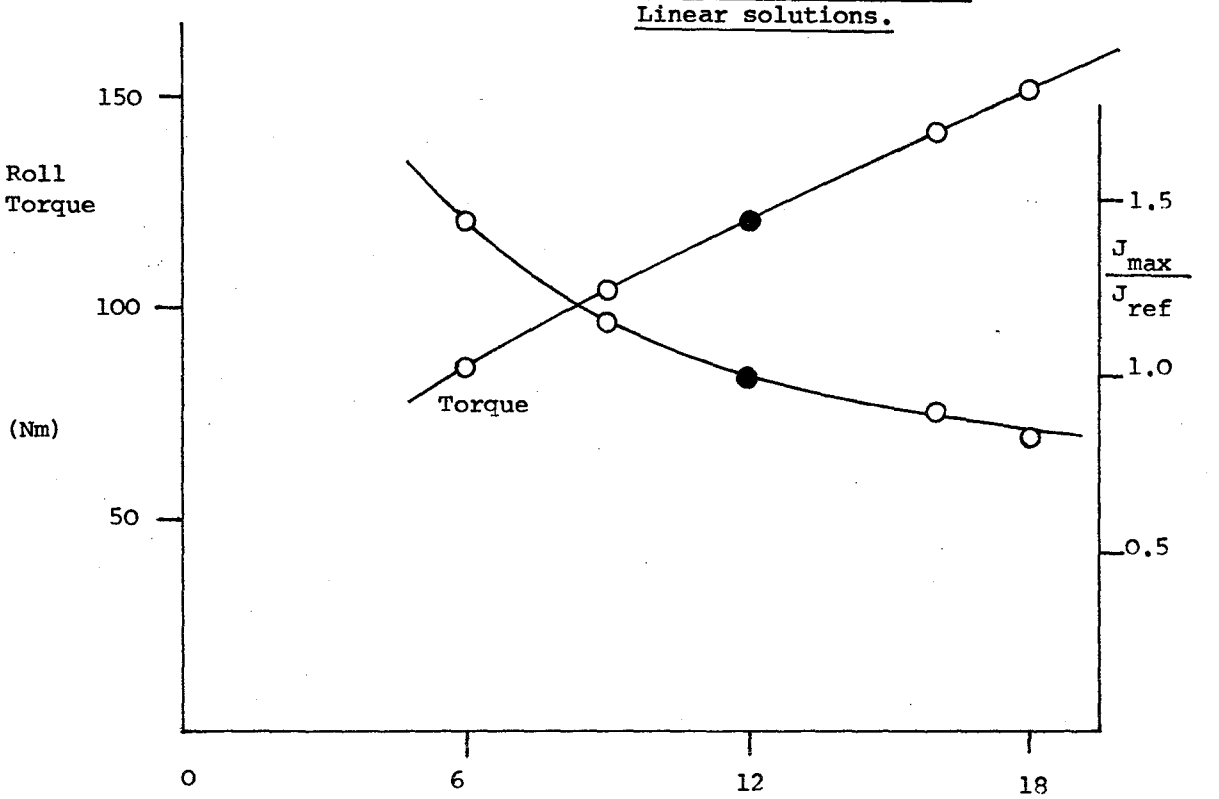

Fig.21 Torque versus chord showing peak induced magnetization. As Fig.18

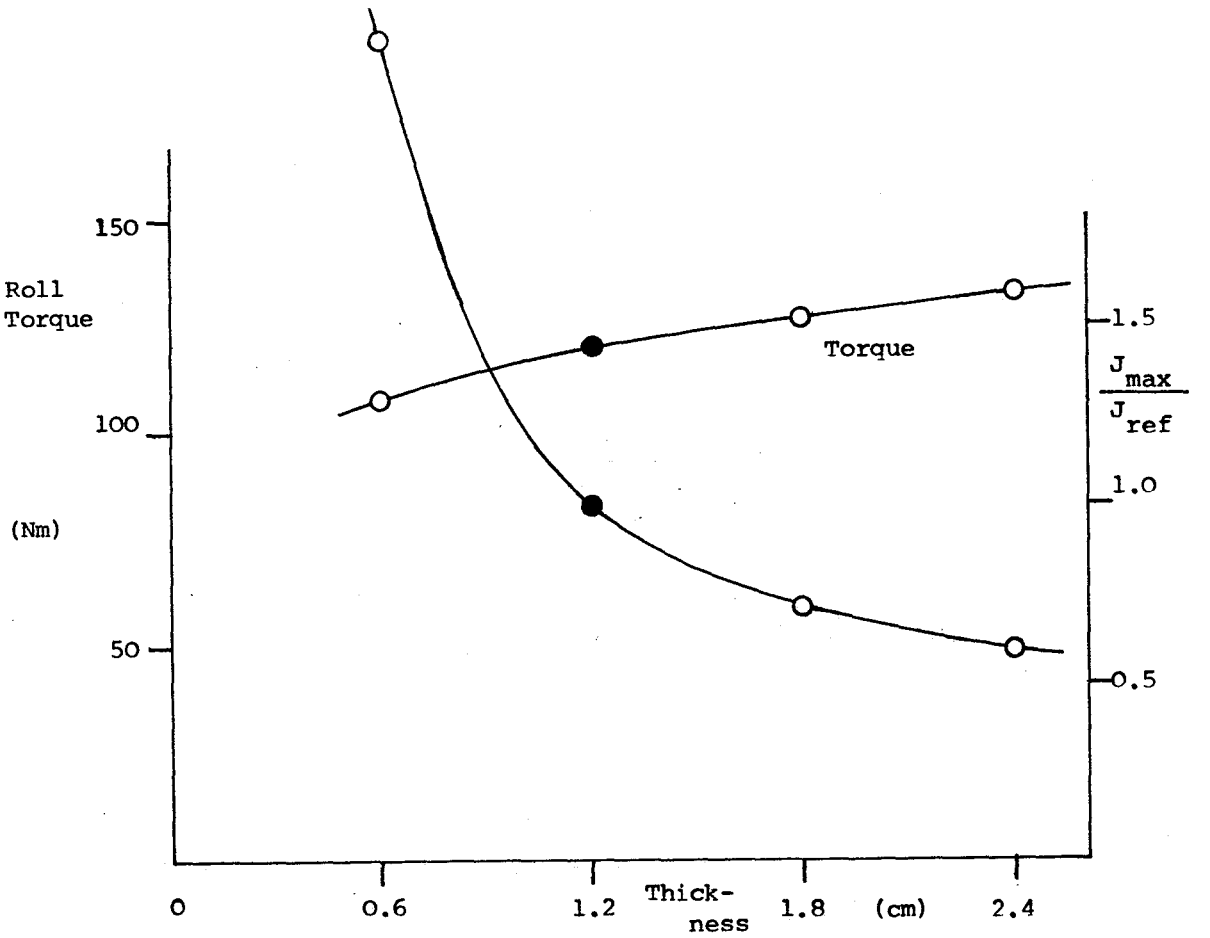

Fig.22 Torque versus thickness showing peak induced magnetization.
As Fig.19

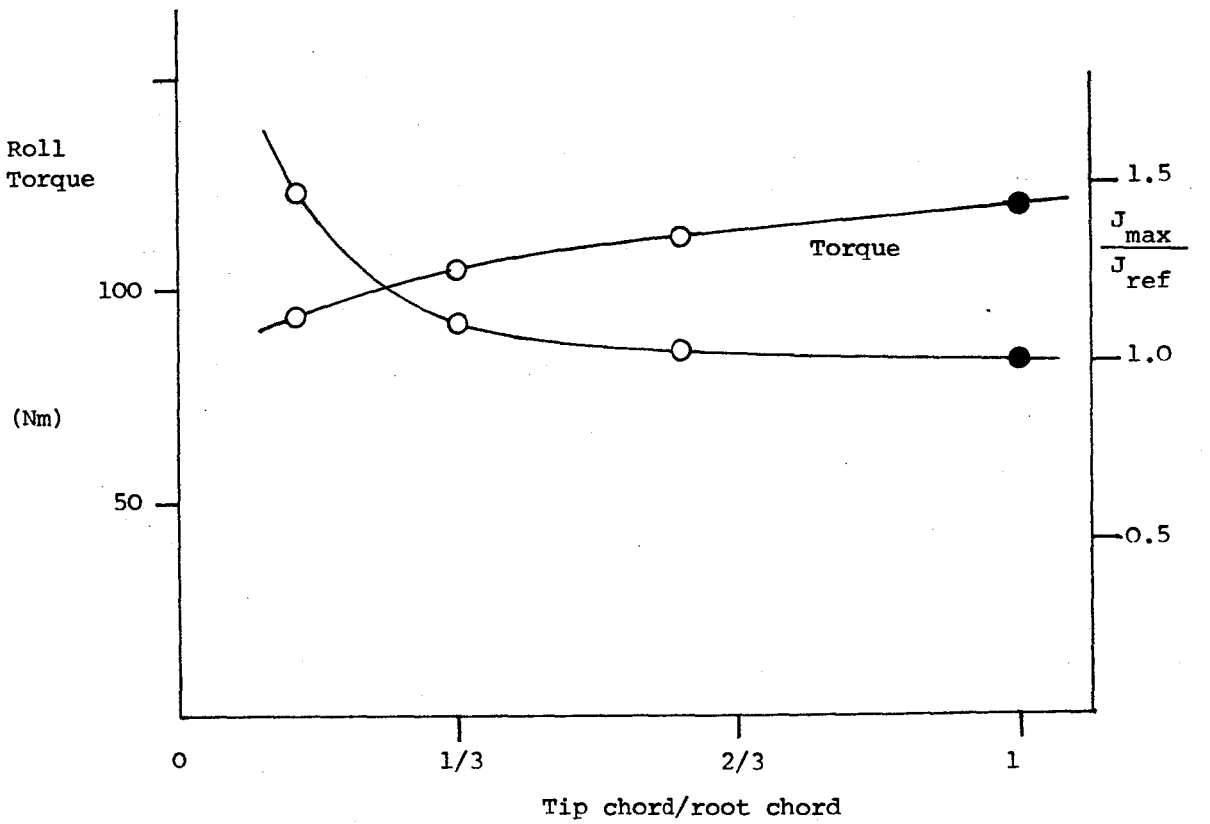

Fig.23 Torque versus taper showing peak induced magnetization.
As Fig.20

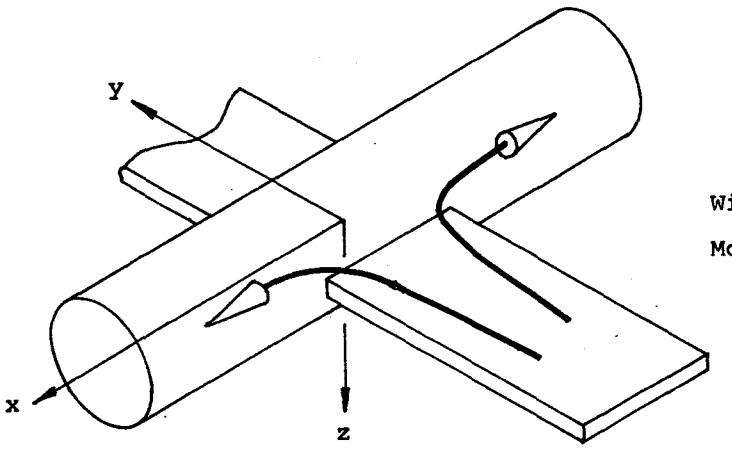

With fuselage

Most flux carried into fuselage core.

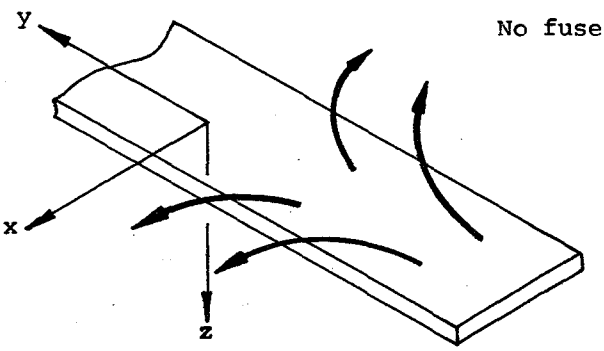

No fuselage. Flux carried through air.

Fig. 24 Easy flux path at wing root with fuselage.

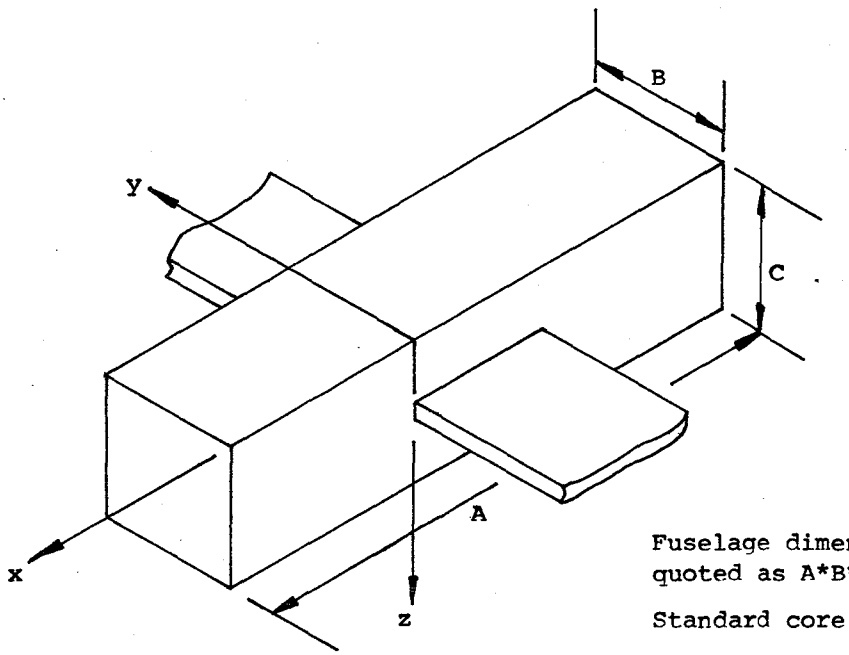

Fuselage dimensions quoted as A*B*C (cm)

Standard core 50*7.4*7.4

Fig. 25 Standard dimensions of fuselage core.

fuselage may or may not act similarly. With the fuselage geometry as defined in Figure 25, the wing core span remains unchanged, the root now being enveloped by the fuselage core. The table below shows some results for this geometry, confirming the expectation of augmentation of torque with fuselage present. The effects appear weak.

Fuselage Dimensions (cms)	Torque (Nm)
Absent	109.78
50 x 5.2 x 5.2	110.22
50 x 7.4 x 7.4	113.53
100 x 7.4 x 7.4	114.40

If a soft iron fuselage core is used it will generally require an axial magnetizing field. The effect of an axial field on the wing cores will tend to be to rotate the spanwise magnetization vectors in the plane of the wing, in the sense of sweepback or sweepforward. Where the core permeability is constant, the magnitudes of the spanwise components will be unaffected. A reduction in the spanwise components, hence torque, will be expected where the wing core permeability is falling with rising magnetization. With the fuselage dimensions fixed at 50 x 7.4 x 7.4 cms (Figure 25) and a near uniform axial field applied by a large Helmholtz coil pair of otherwise arbitrary dimensions this expectation is confirmed by the results shown in Figure 26.

The magnitude of the axial magnetization components induced in the wing core by the axial field will depend to a large extent on the axial slenderness of the core, which will in turn be most strongly affected by the cores thickness to chord ratio, relatively thick, narrow chord cores being least powerfully affected. Very thin cores, such as the F-16 case studied later, may this be seriously affected although no relevant data currently exists.

3.4. Effect of sweepback

Sweepback of the wing cores as defined in Figure 27 rotates the easy axis of wing core magnetization away from the spanwise direction, but does not affect

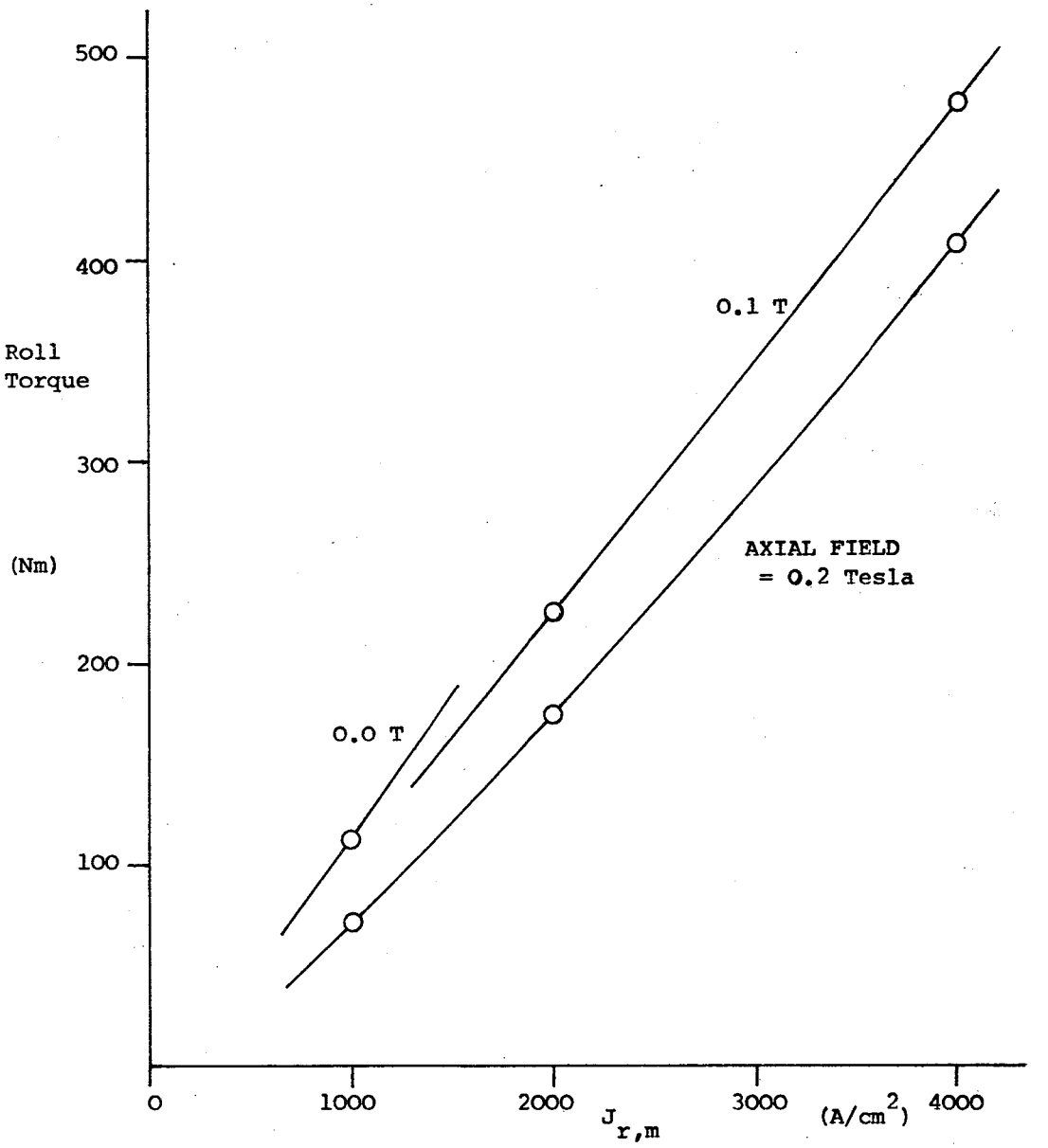

Fig. 26 Torque versus $J_{r,m}$. Baseline core with fuselage as Fig.25

Baseline E/Ms. 5 point BH curve.

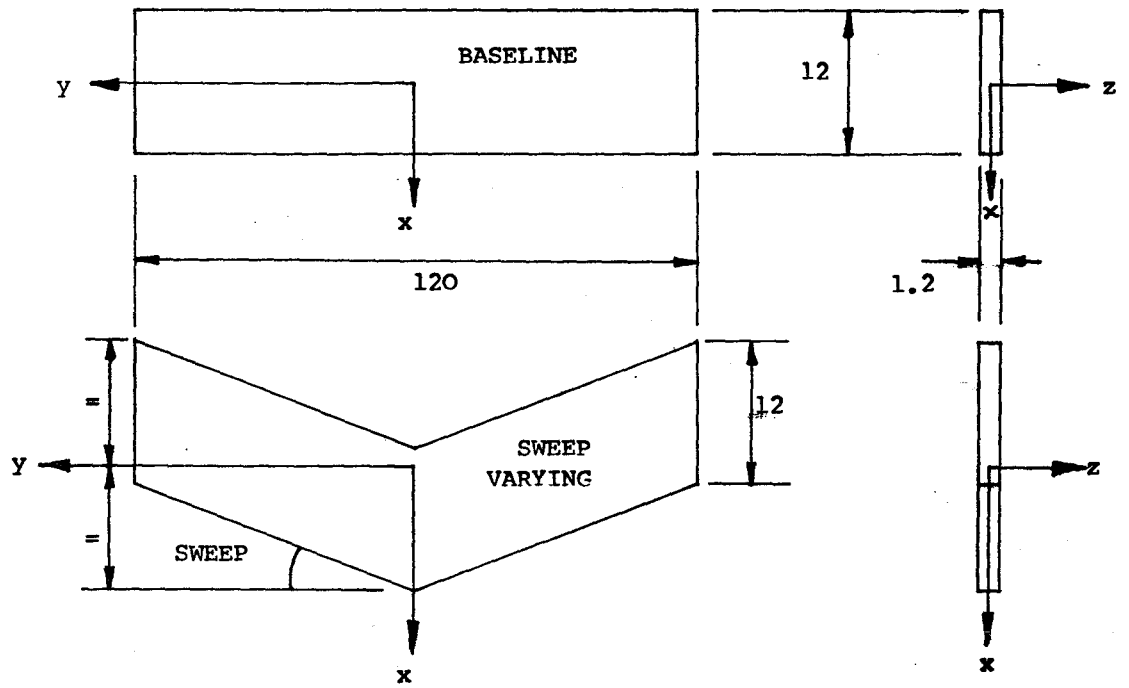

Fig.27 Definition of sweepback. All dimensions cms.

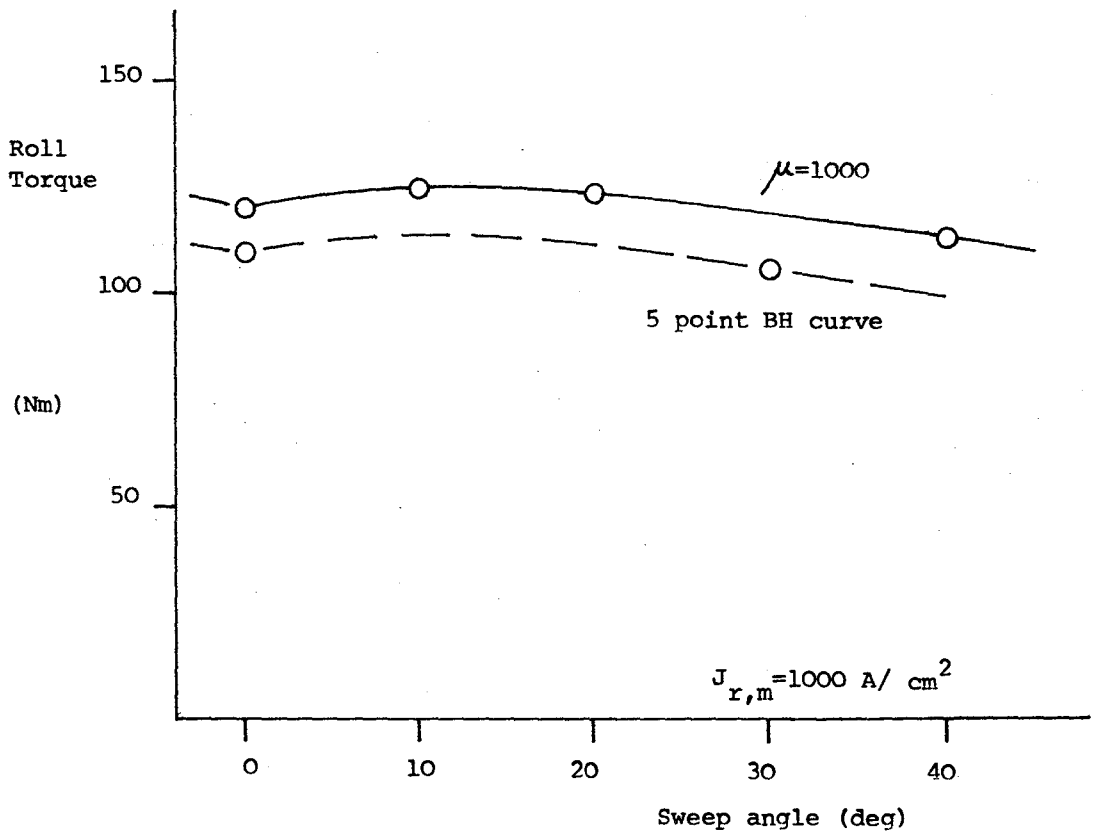

Fig.28 Torque versus sweep angle. Baseline E/Ms. Core as Fig.27

the core volume nor the position of the centroid of volume. The induced magnetization vectors with a purely spanwise magnetizing field are thus expected to themselves be sweptback, at some angle probably less than the geometrical sweep angle. This would be expected to lead to lower torque per unit applied field in general. However, at low sweep angles it would appear that the increasing slenderness of the core, caused by the chosen geometry, dominates, leading to slightly augmented torques at modest sweep angles, as shown in Figure 28.

When an axial magnetizing field is applied, components of that field act along the easy axis of magnetization of the sweptback core, increasing or decreasing the spanwise magnetization components (hence torque) depending on the field polarity. For a sweep angle of 30 degrees Figures 29, 30 show the effect to be significant. At relatively low spanwise fields it is seen that powerful axial fields of either polarity reduce the torque for particular spanwise and through-wing field levels.

3.5. Behaviour at high levels of roll torque generating field.

At high applied roll field levels the core becomes saturated over most of the volume. The induced magnetization components then behave as vectors of constant strength but variable direction. It is not immediately obvious whether, under these conditions, increases in applied field should lead to increases in torque generated and, indeed, whether or not some absolute maximum torque capability exists for each particular core geometry.

Preliminary analytic studies of an idealised magnetostatic configurations (ellipsoid in uniform field) suggest that an absolute maximum should exist and that this maximum can be realised with finite applied fields of appropriate sense and direction.

Various high applied field cases have been computed with GFUN (Figures 31, 32) with somewhat inconclusive results. It should be noted here that the torque integration schemes in GFUN became progressively less reliable at increasing applied field levels. This is due to the difficulty of accurately resolving on the surface of the external control volumes (Section 2.1, Figure 7 and (8)) the "model" field (due to the core's induced magnetization and now of essentially fixed magnitude) from the total field, which becomes mostly due to the applied field from the E/Ms.

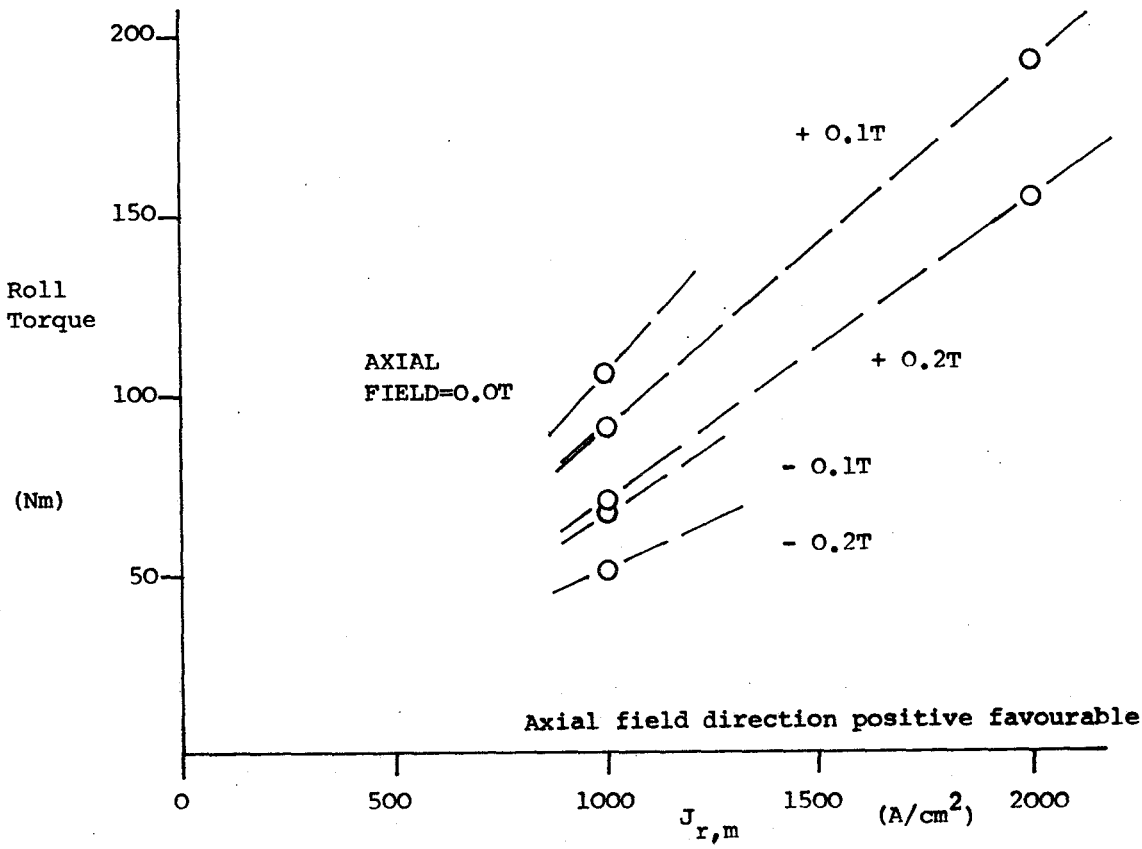

Fig.29 Effect of axial field on sweptback core. Baseline E/Ms. Core as Fig.27. Sweep=30 . 5 point BH.

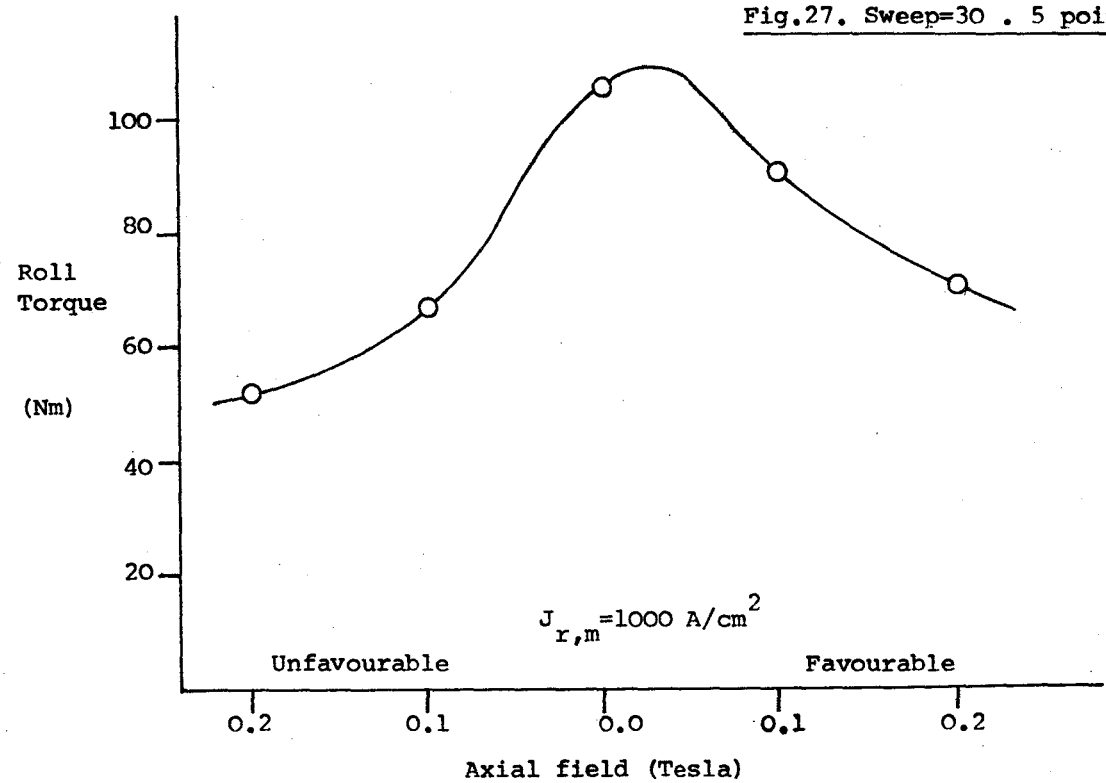

Fig.30 Effect of axial field on sweptback core. Baseline E/Ms. As Fig.29

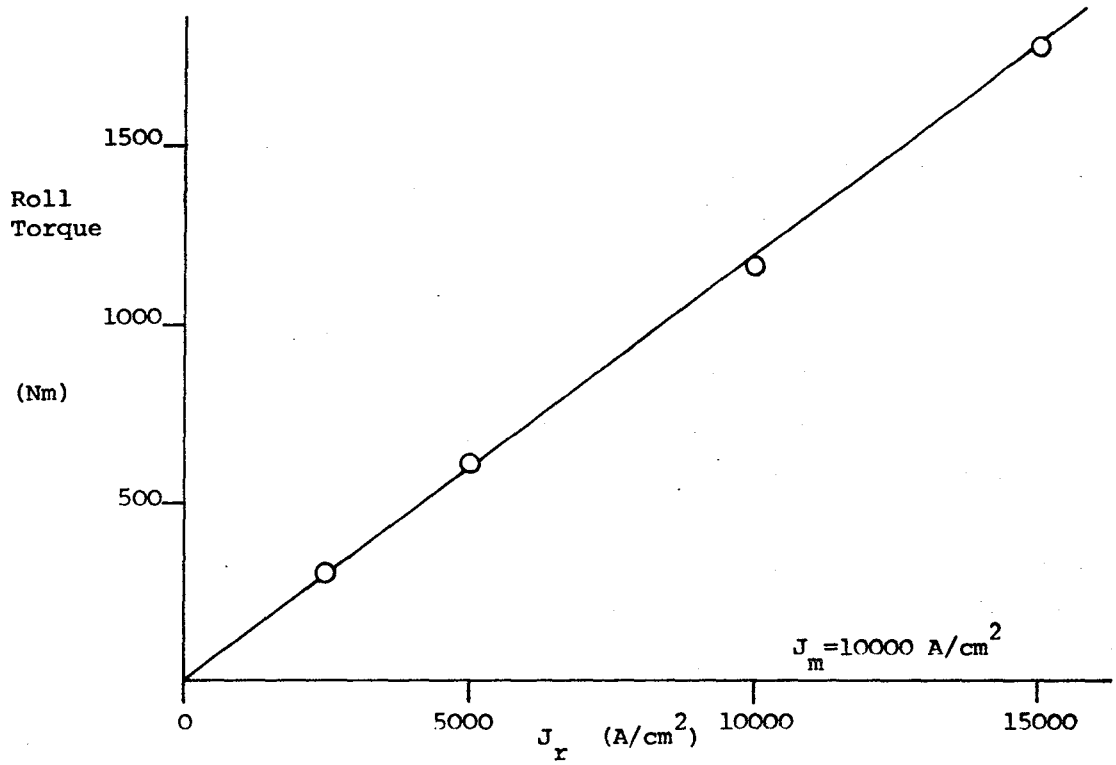

Fig.31 Torque versus J_r, J_m constant. High applied field levels. Baseline E/Ms. Baseline core. 5 point BH curve

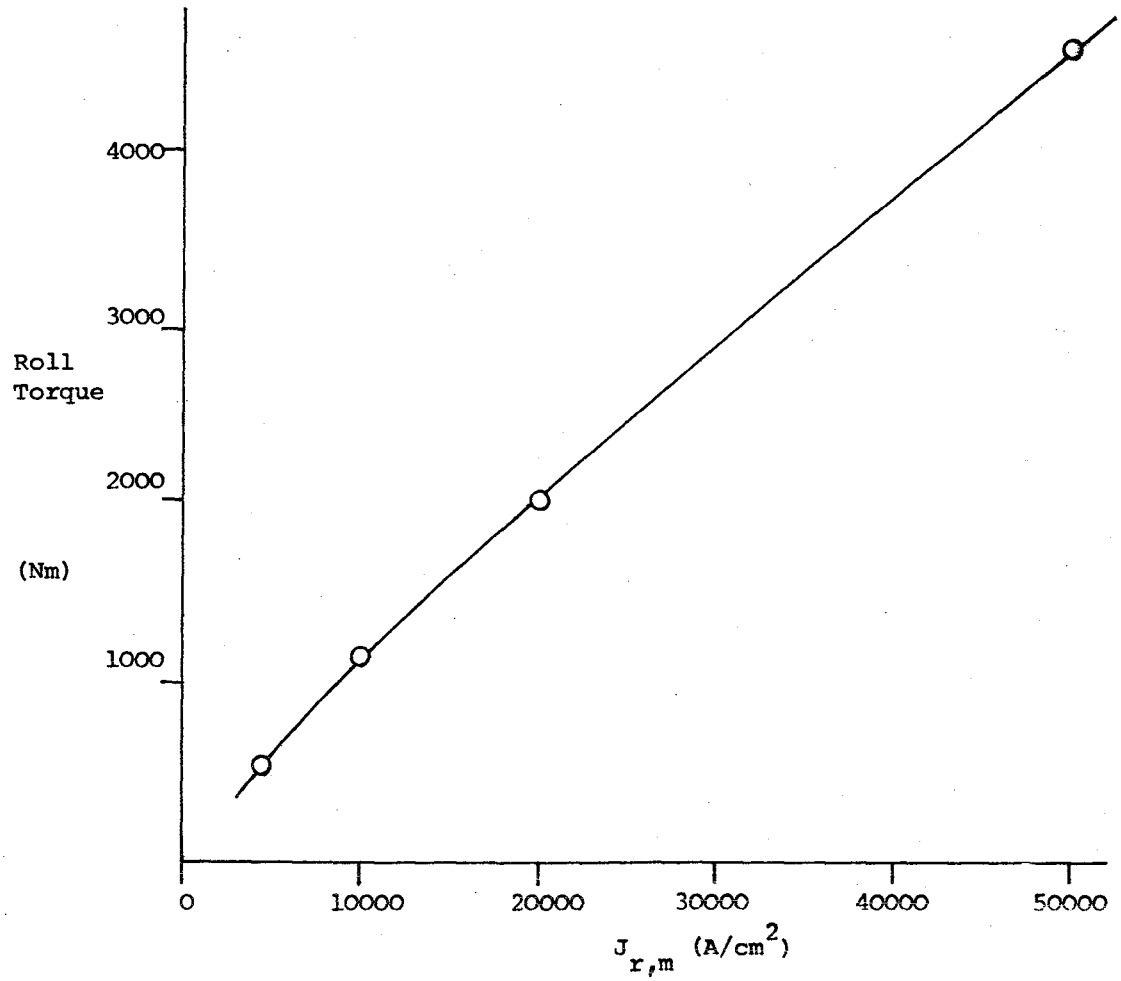

Fig.32 Torque versus $J_{r,m}$. Baseline E/Ms and core. 5 point BH curve.

The peak torque levels achieved in Figures 31, 32 are, however, at least one order of magnitude in excess of apparent existing LMSBS requirements [9].

3.6. Pseudo F-16 wing core performance

It is understood that a representative aircraft type for use in LMSBS design studies has previously been chosen to be the F-16 fighter. This type presents a considerable challenge to the SIM roll scheme since it's wing thickness (hence volume) is very low, the blockage effects of the fuselage necessitate choice of model wingspan considerably below the 50% of test section width used heretofore and the extreme taper both in chord and thickness leaves relatively little volume in the magnetically most effective tip regions.

Each wing panel has been crudely represented with GFUN as a hexahedral slab, uniformly tapered in both thickness and chord, with approximately the same span, total core volume and moment of volume about the chordwise centroids of volume as a typical F-16 model (Figure 33). The element distribution, particularly the element aspect ratio, within the core is at the limits of what is generally acceptable with GFUN, hence the results must be regarded as subject to increased uncertainty (Section 4.3) but again comfortably exceed apparent LMSBS requirements [9] at moderate applied field levels (Figures 34, 35, 36, 37).

3.7. Effect of variations of E/M geometry

Non-circular E/Ms, for instance those in Figure 38, exhibit improved packing around the wind tunnel test section compared to the circular baseline E/Ms. The field distribution in the region of the model will be altered also, although the effect tends to be slight due to the relative remoteness of the E/Ms. The performance of different E/M configurations may be approximately normalized by an appropriate measure of the field in the region of the model, but calculated with the model absent. This has been done by computing the mean field level along the y axis, taken over the span of the model. It is seen in the tables below that the effect of E/M geometry on the generated torque is small.

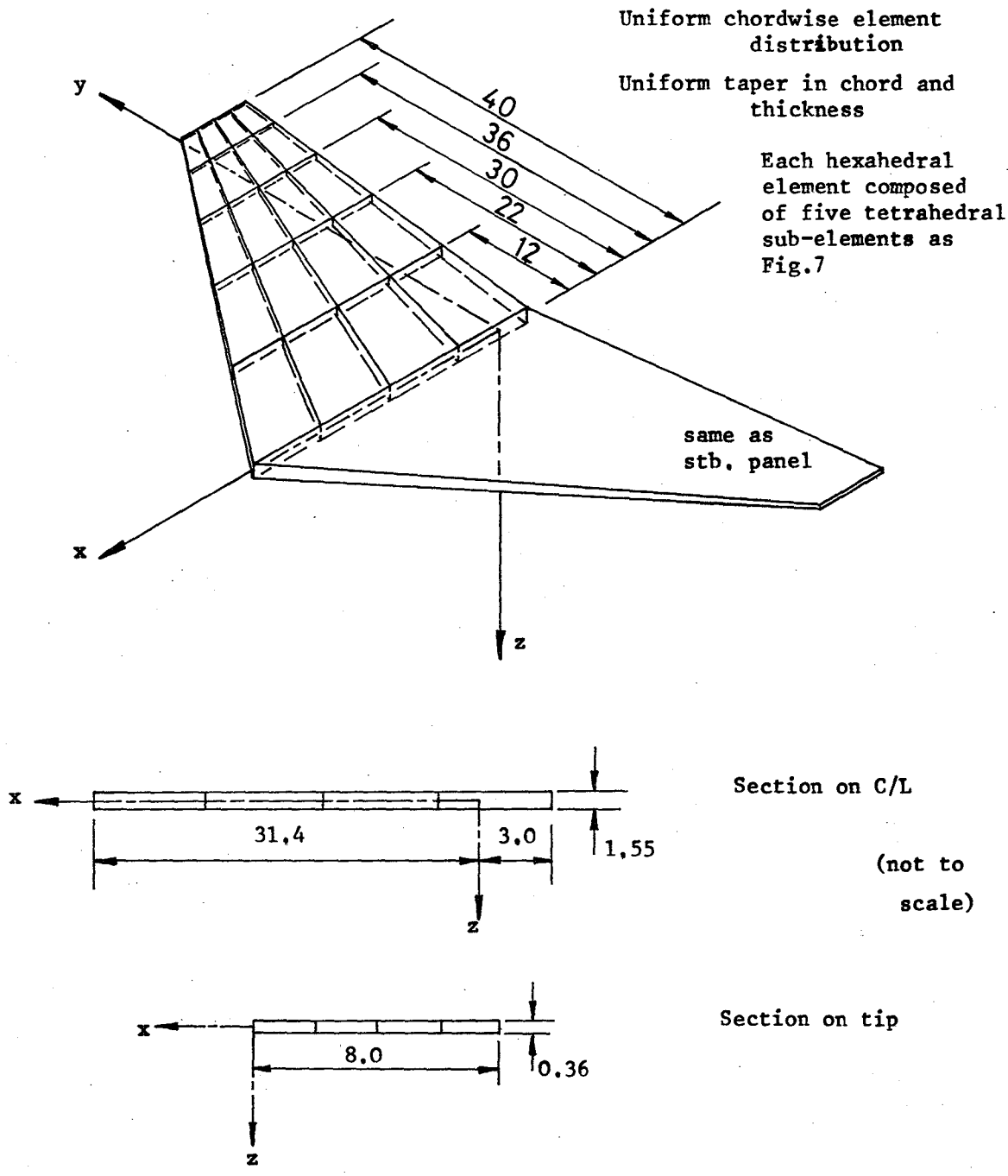

Fig.33 "F-16" slab core geometry. All dimensions in cms.

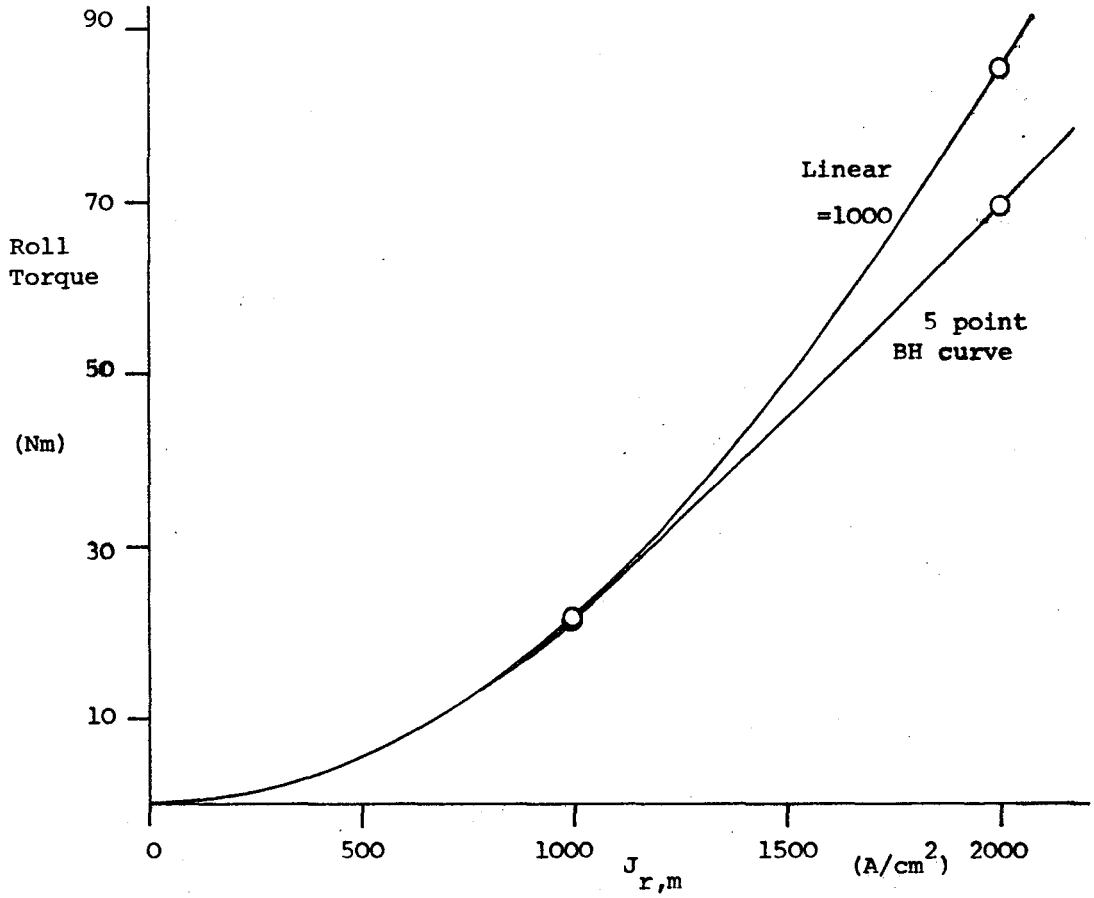

Fig.34 Torque versus $J_{r,m}$. Baseline E/Ms. "F-16" core geometry.

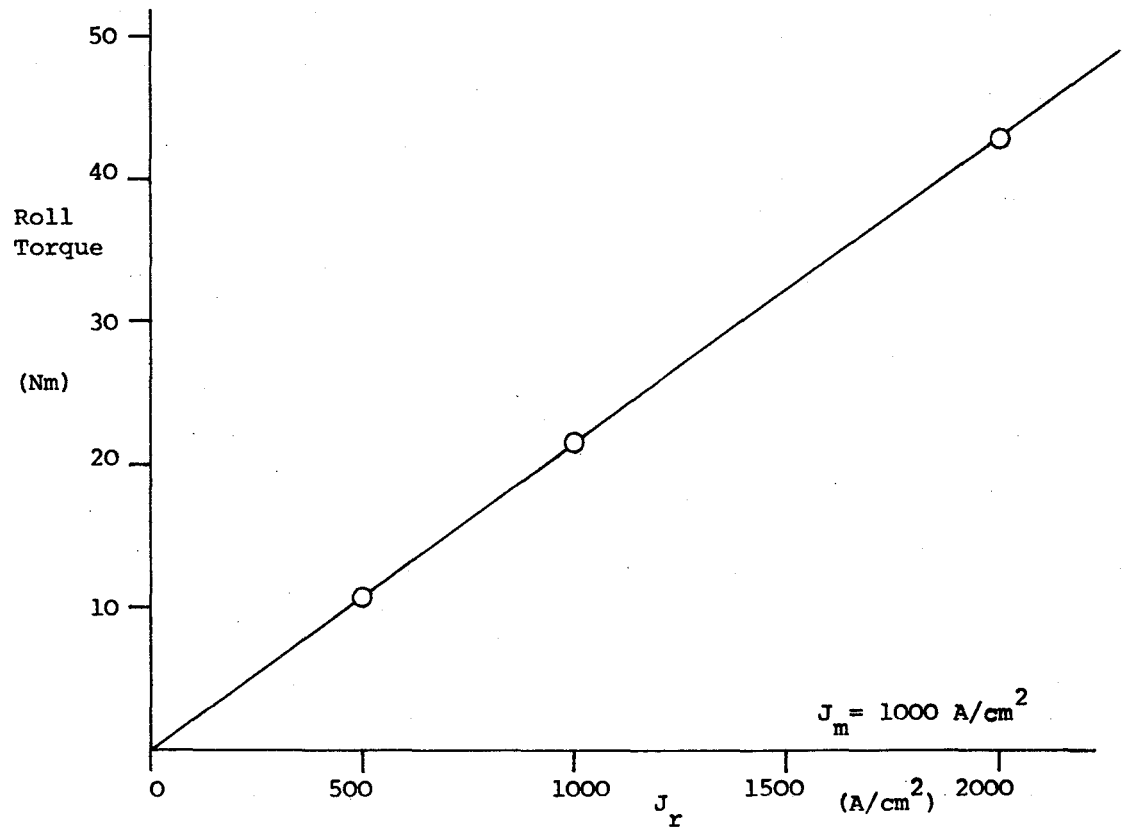

Fig.35 Torque versus J_r, J_m constant. Baseline E/Ms. "F-16" core geometry.

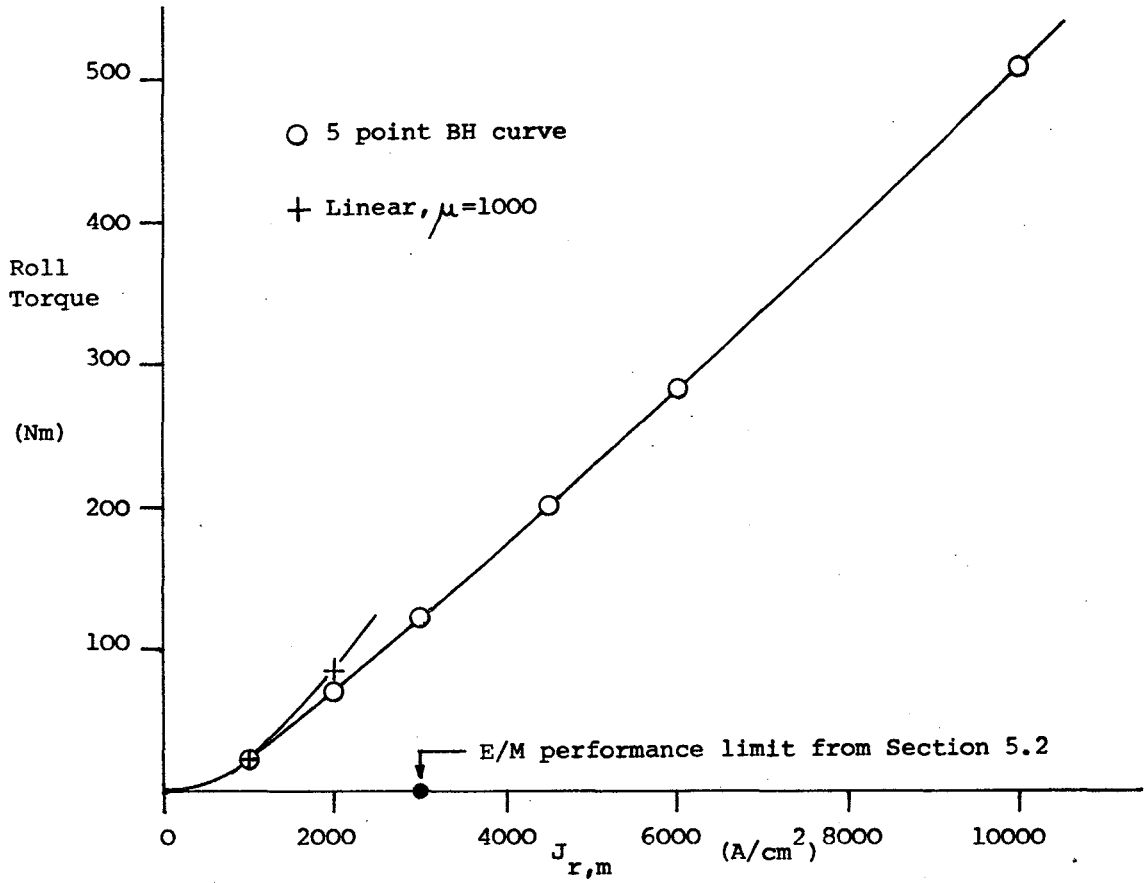

Fig.36 Torque versus $J_{r,m}$. Baseline E/Ms. "F-16" core geometry.

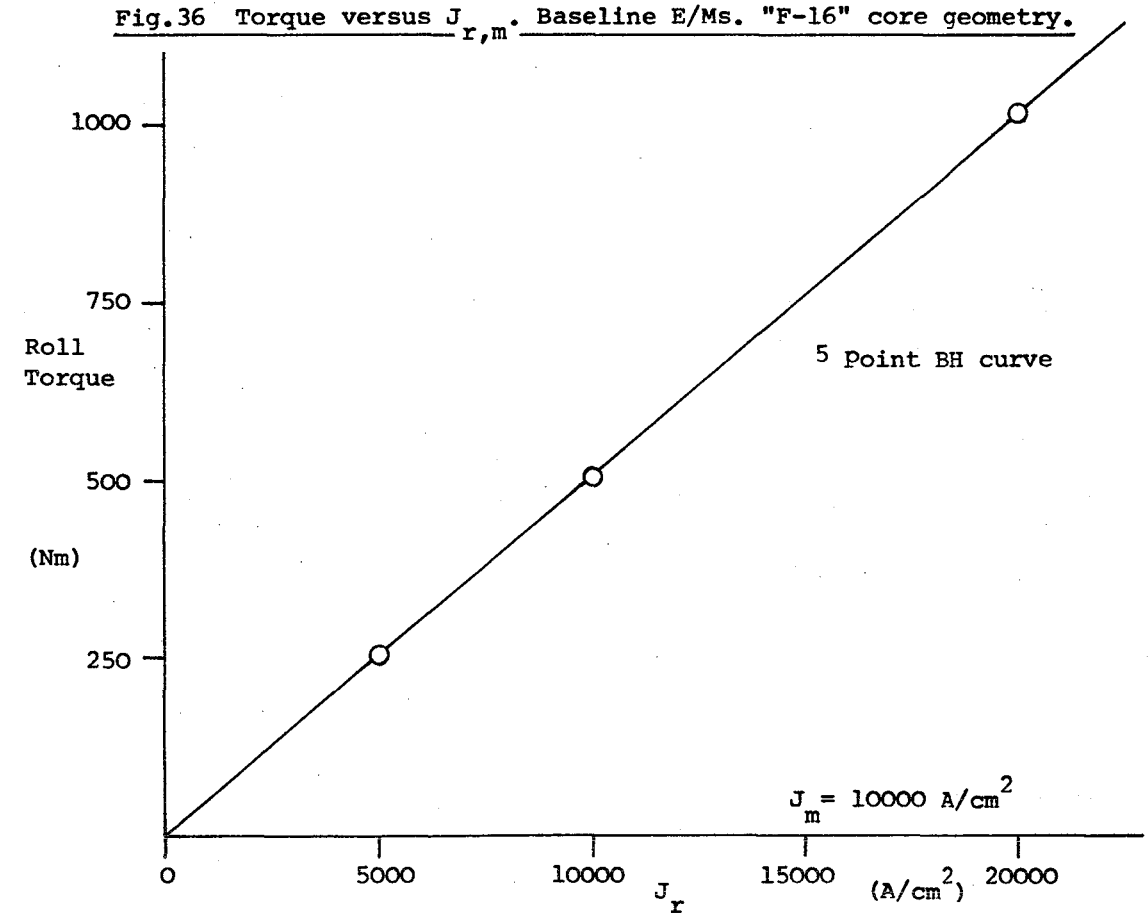

Fig.37 Torque versus J_r, J_m constant. Baseline E/Ms. "F-16" core

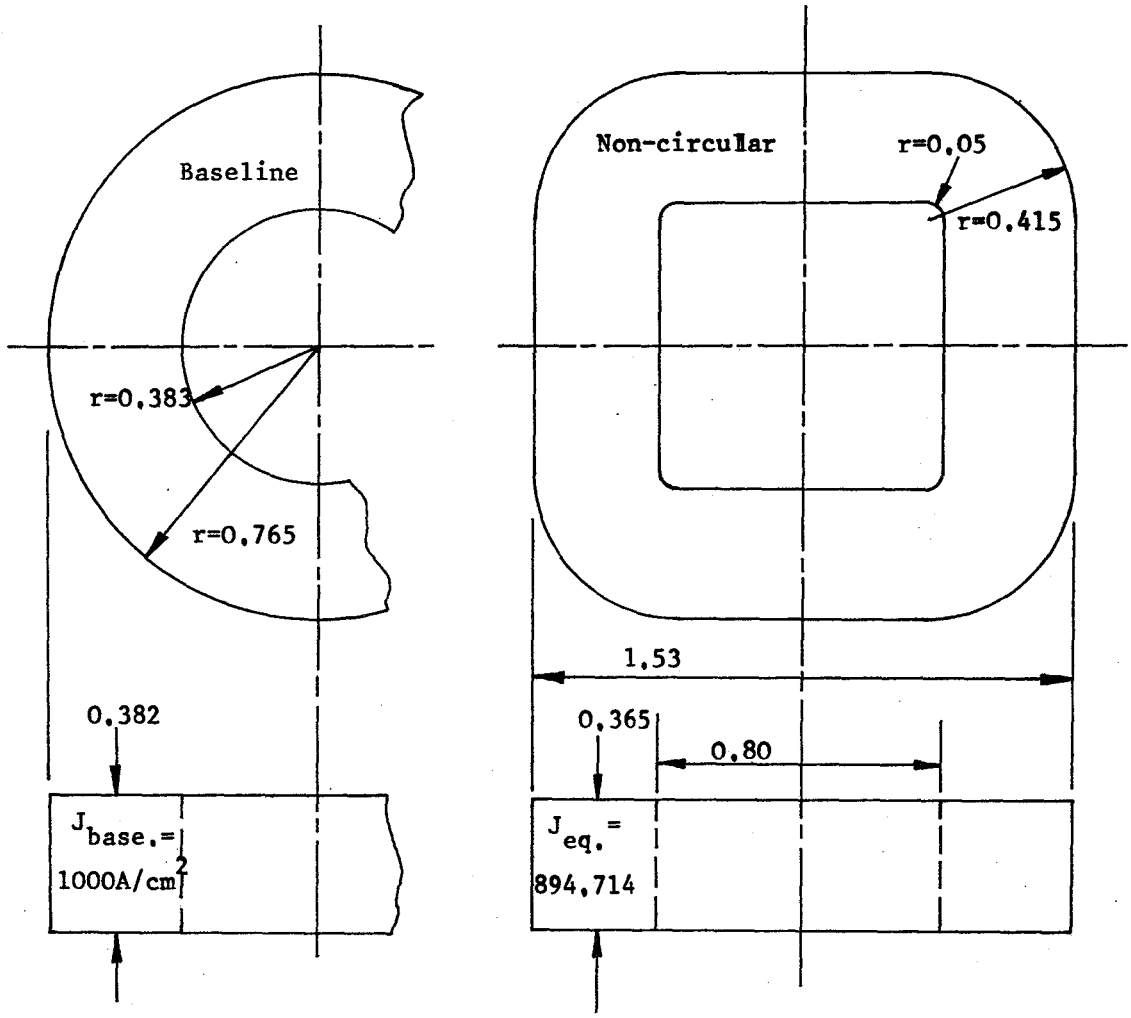

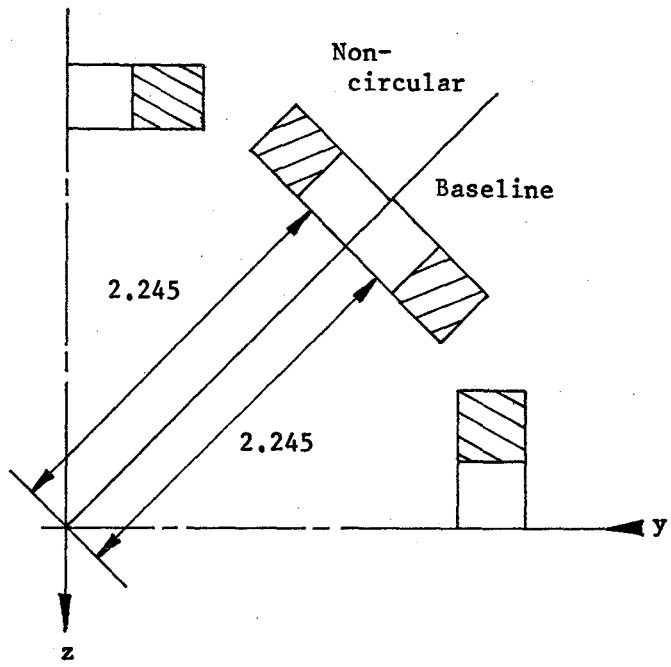

J in non-circular E/Ms corrected to approximate baseline field in region of baseline model.

Fig.38 Comparison of baseline and equivalent non-circular E/M geometry.

Dims. in metres.

E/M geometry	Normalised $J_{r,m}$	Torque (μ = 1000)
Figure 6	1000.0	120.51
Figure 38	894.97	119.78

For reasons other than production of rolling moments, the classical array of 8 E/Ms distributed in the yz plane may not be preferred. A 16 E/M system, shown in Figure 39, has therefore been computed as an example with E/M performance normalized as above:

E/M geometry	Normalized $J_{r,m}$	Torque (μ = 1000)
Figure 39	869.65	112.82

It is clear that the performance of the SIM system is not strongly affected by the detail geometry of the E/Ms, hence permitting consideration of alternative E/M geometries and configurations with the existing GFUN results being approximately applicable provided E/M performance is normalized by the models near field using Figure 40.

4. VERIFICATION OF GFUN DATA

4.1. Alternative torque computations

No direct alternative computations of the performance of any representative SIM system have been attempted since this would necessarily require access to an alternative computer program of comparable power and sophistication to GFUN, preferably solving the magnetostatic system by an entirely different method. Such programs probably do exist.

However, as mentioned earlier, the reliability of GFUN's prediction of magnetization of iron regions has been good for many years and there seems no particular reason to regard the computed wing core magnetizations as being subject to any more than the usual levels of uncertainty (8). Were this the only source of uncertainty, the computed torques could be regarded as likely to be accurate, within the limits of geometrical and other assumptions, to plus or minus

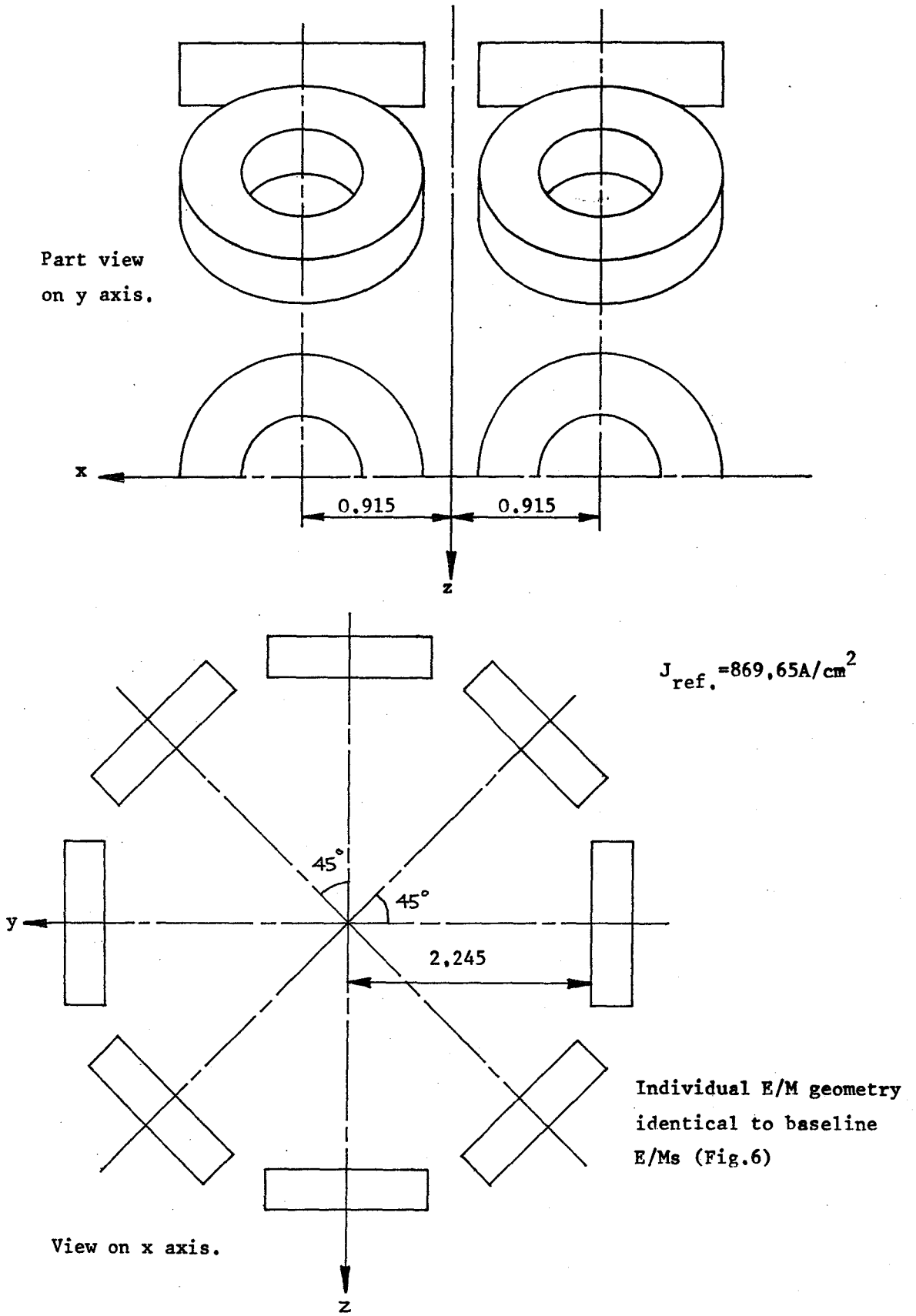

Fig.39 16 E/M roll geometry and configuration. Dims. in metres.

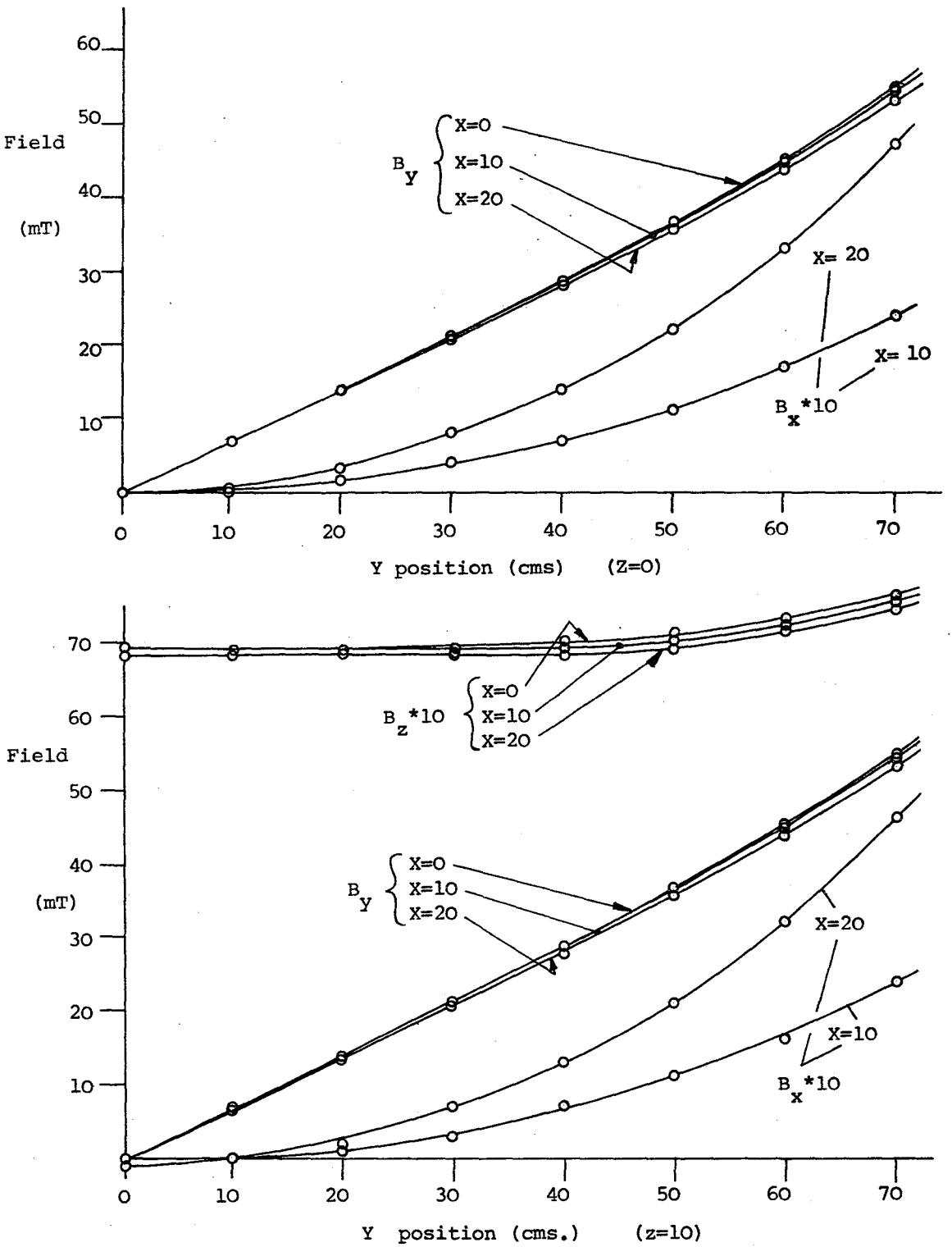

Fig.40 (A) Near field of baseline magnetizing E/Ms @ $J_{r,m}$=1000A/cm^2

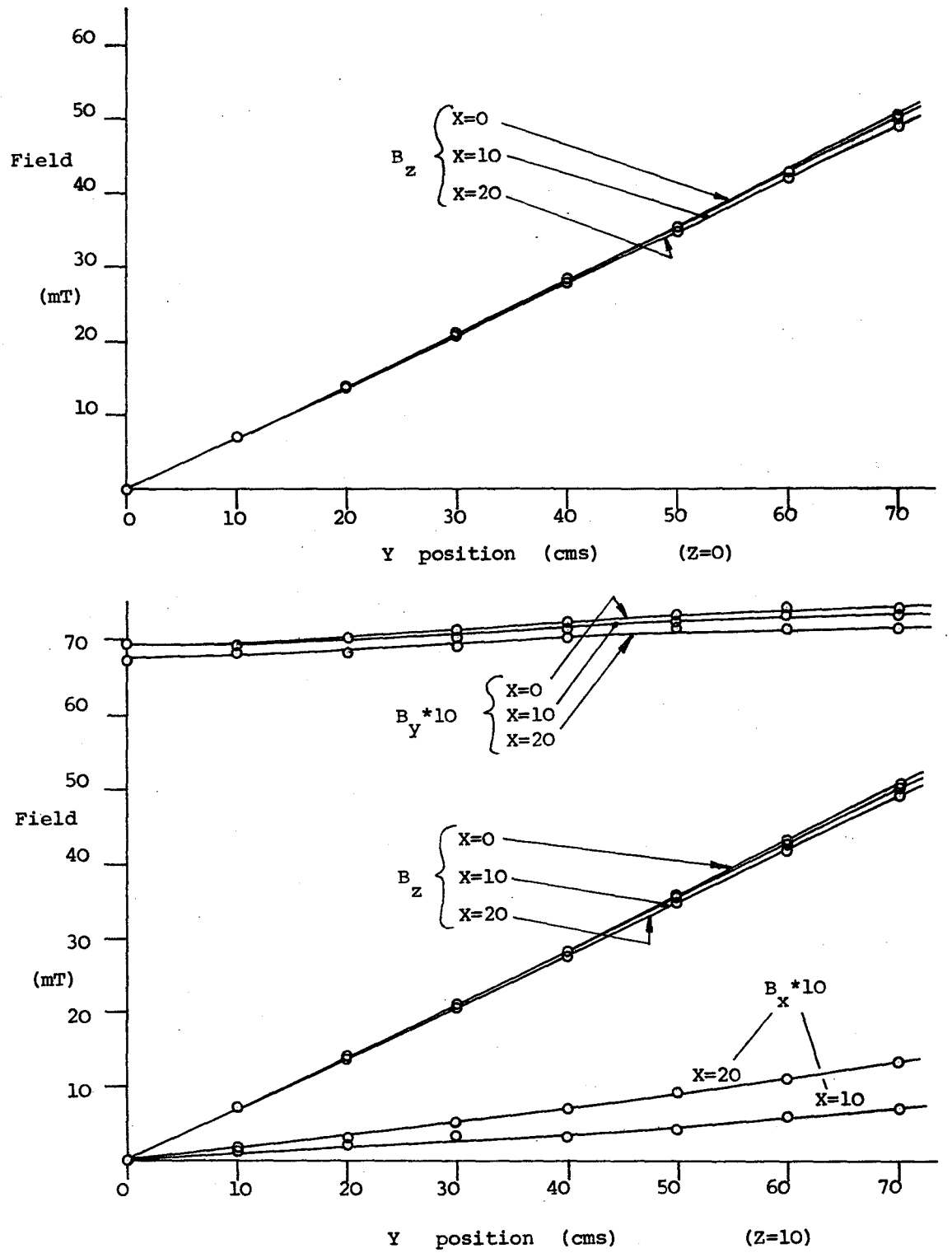

Fig.40 (B) Near field of baseline "roll" E/Ms @ $J_{r,m}$=1000A/cm^2

very few percentage points at all computed applied field levels for the baseline and similar geometries, with somewhat greater uncertainty in certain cases, such as the F-16 core, where the iron element distribution was sparser than desirable (see Section 4.3).

The main potential source of uncertainty must be regarded as the torque integration schemes themselves, since these have been specially developed for the SIM computations and hence not subject to such extensive testing and verification as the rest of GFUN.

It is possible with GFUN to arbitrarily fix the induced magnetization in iron elements, thus effectively converting them to permanent magnet material. If this is done in such a way as to approximately preserve the typical spanwise magnetization in the SIM cores (Figure 41) then direct and representative verification of the torque integration schemes is possible. Alternative calculations have made using the Southampton University program FORCE (derived in part from the MIT program TABLE) which calculates forces and torques by elementary numerical integration of the relevant vector products of applied field and core magnetization over the volume of the core. This method differs fundamentally from the methods used in GFUN. Results for the geometry of Figure 41 are as follows:

Torque integration scheme	Predicted Roll Torque (Nm)
GFUN by Maxwell field stress integration over surfaces of external control volume ± 70 x 20 x 10 cms	113.94
FORCE by vector product integration over volume of core	116.82

The discrepancy of approximately 2.5% is considered acceptable though leaving scope for future improvement.

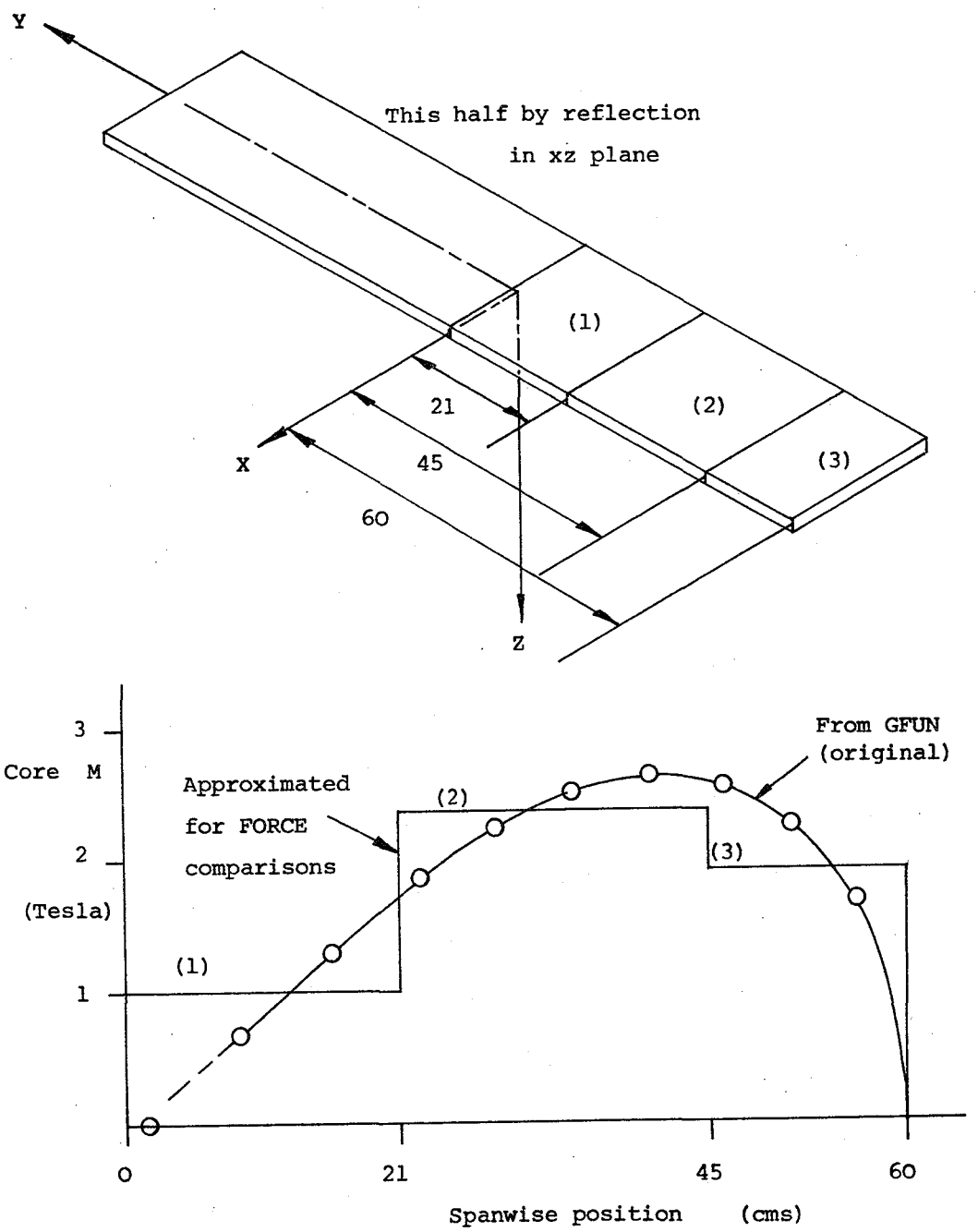

Fig.41 Approximate spanwise magnetization distribution for comparison of GFUN and FORCE torque integration schemes.

Certain comparisons have been made of predicted torques over differing GFUN control volumes with typical results as follows:

GFUN control volume dimensions (cm)	Relative torque to standard volume
± 70 x 20 x 10 (assuming symmetry in the yz plane)	1.0
± 70 x 20 x 10 (no symmetry)	0.999993
± 90 x 35 x 25 (yz symmetry)	0.9856

These results are similarly considered acceptable.

As mentioned in Section 3.5 it is thought that the accuracy of the GFUN torque integration scheme will fall with rising applied field level when the SIM cores are well into saturation. No high applied field computations were made with permanent magnet cores specified, and this is a serious ommission but can be rectified by more detailed analysis and computation using existing data.

4.2. Experimental measurements of torque with low applied fields and correlation with GFUN predictions

Experimental verification of the bulk of GFUN's predictions are not possible without an array of powerful (high field) E/Ms. No such facilities were available. However, 8 identical, low field, conventional uncooled copper E/Ms were available from the Southampton University MSBS then undergoing reconstruction (12). These E/Ms were not unfortunately axisymmetric but since it is believed that the SIM system is not particularly sensitive to detail E/M geometry, rather to the mean applied field levels in the region of the SIM cores, representative low field (approximately constant permeability) torque measurements could be made.

The geometry and characteristics of the SIM cores is shown in Figure 42 with the E/M layout indicated in Figures 43, 44. The GFUN representation of the E/Ms was of necessity somewhat idealised (Figure 45) and a correction to E/M current density proved necessary to acheive near-identical field in the region of the model. Presentation of all the experimental data obtained is outside the scope of this report but some performance curves with corresponding

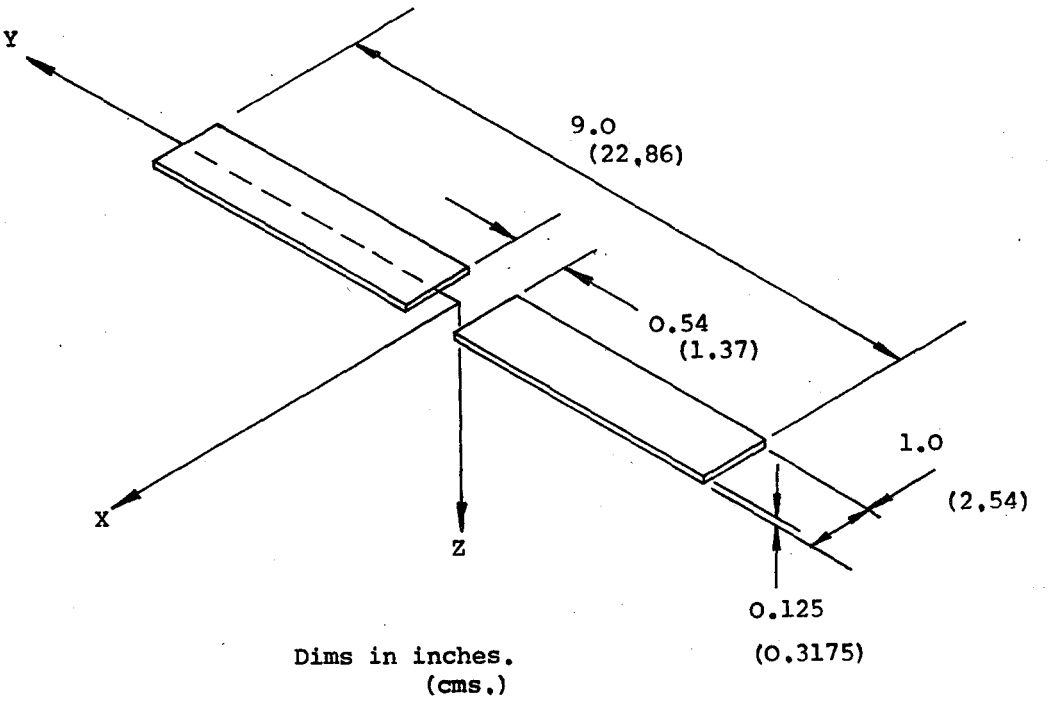

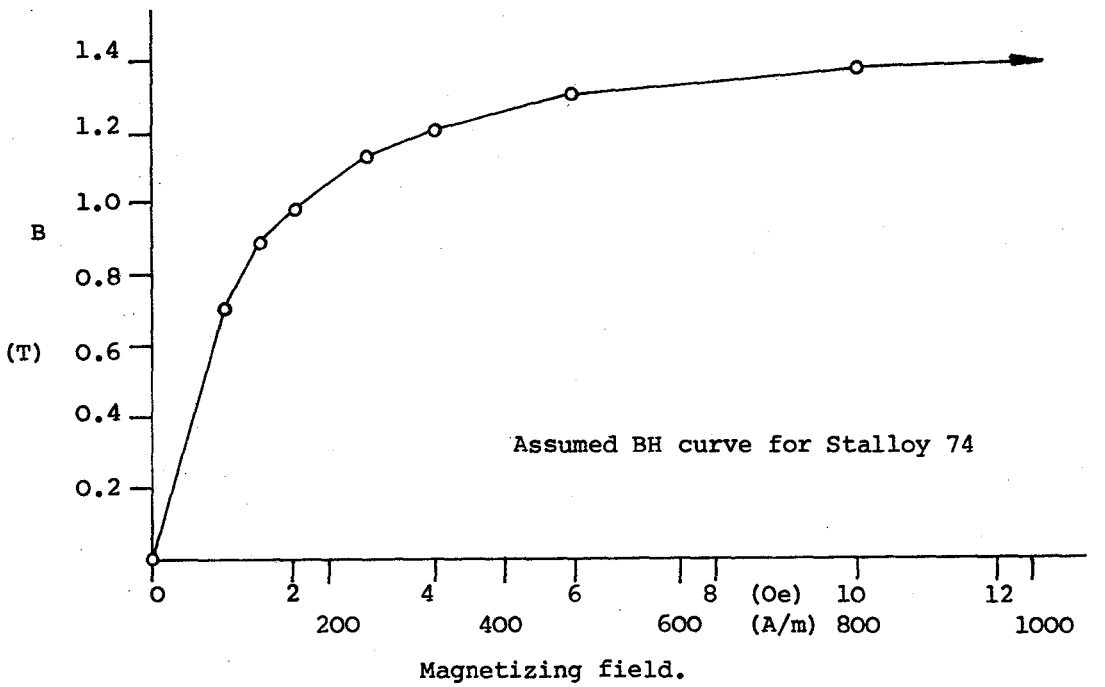

Fig.42 Geometry and characteristics of SIM cores for experimental verification of GFUN predictions.

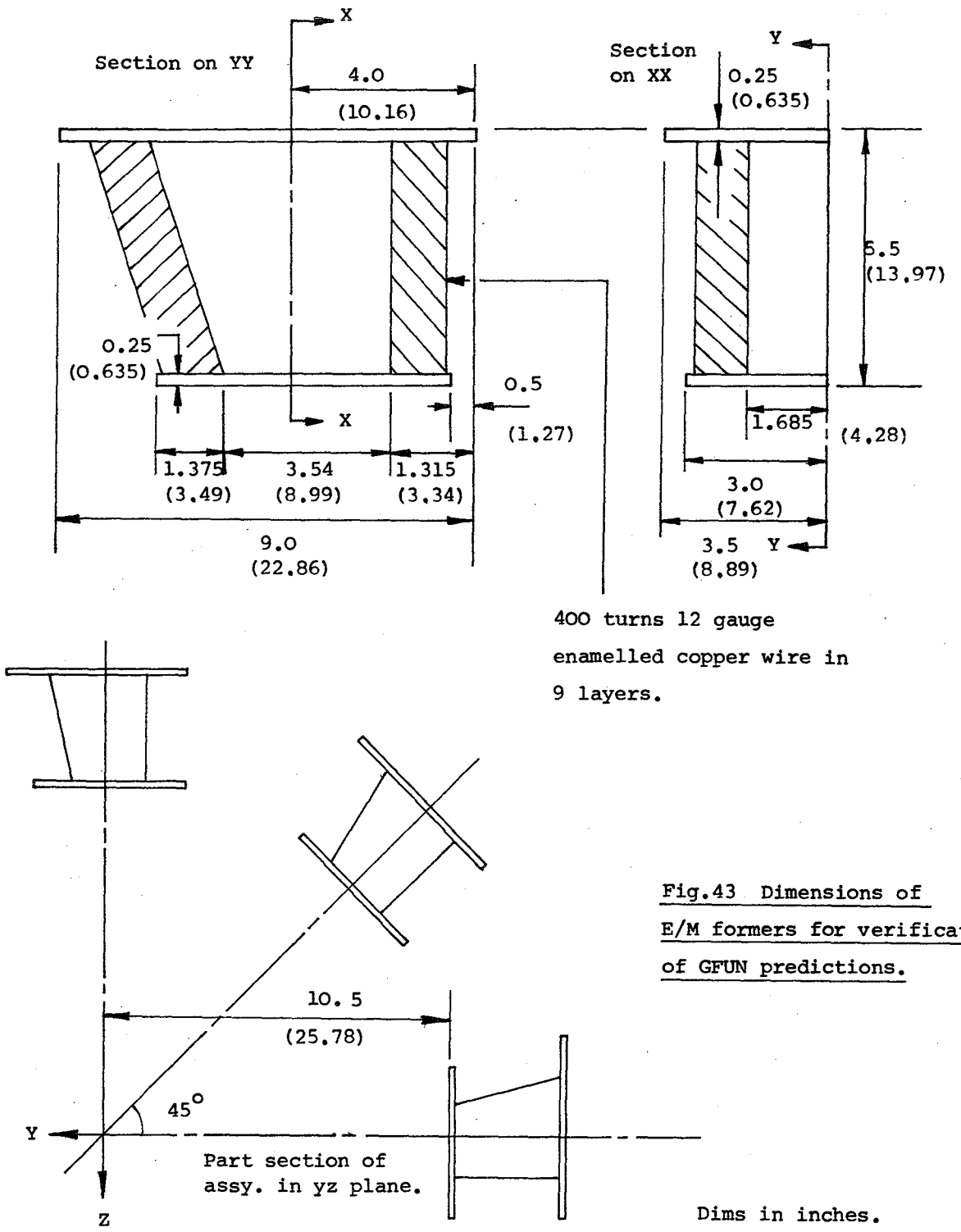

Fig.43 Dimensions of E/M formers for verification of GFUN predictions.

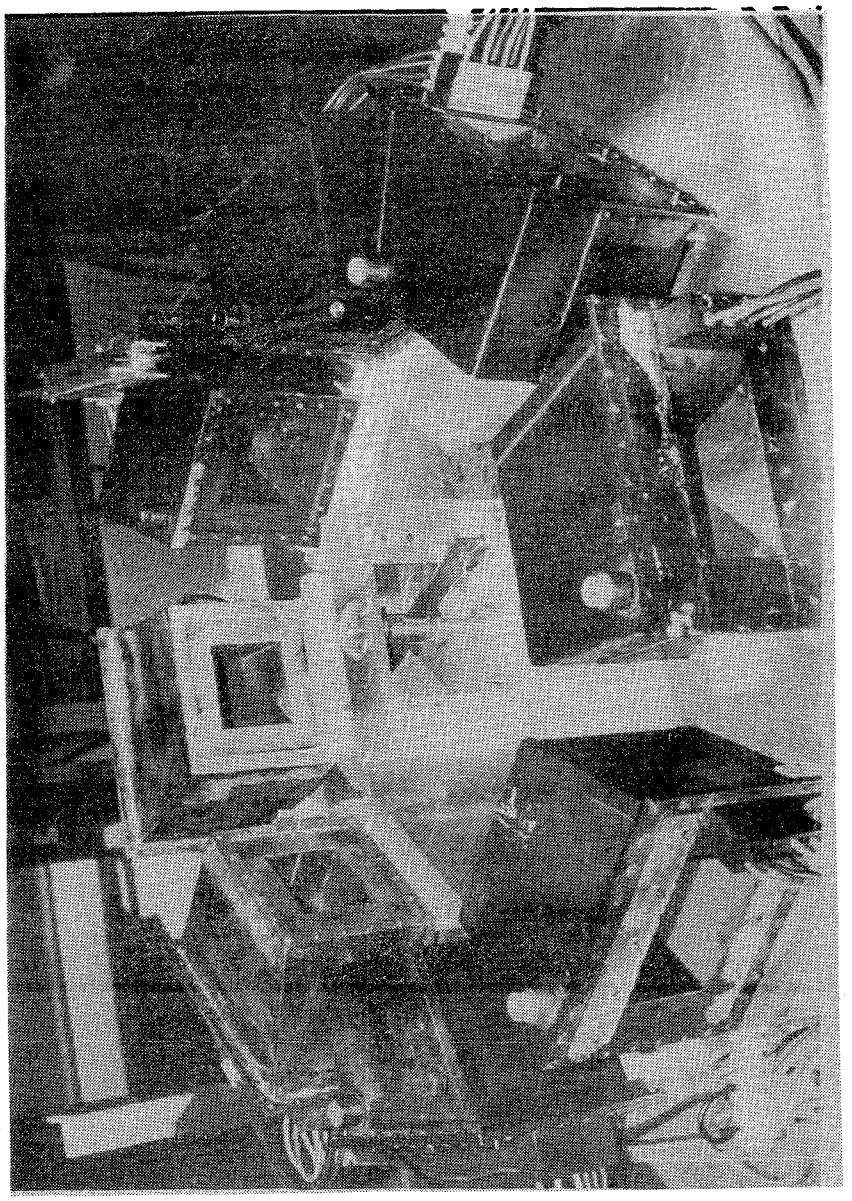

Fig.44 Experimental measurement of roll torque.

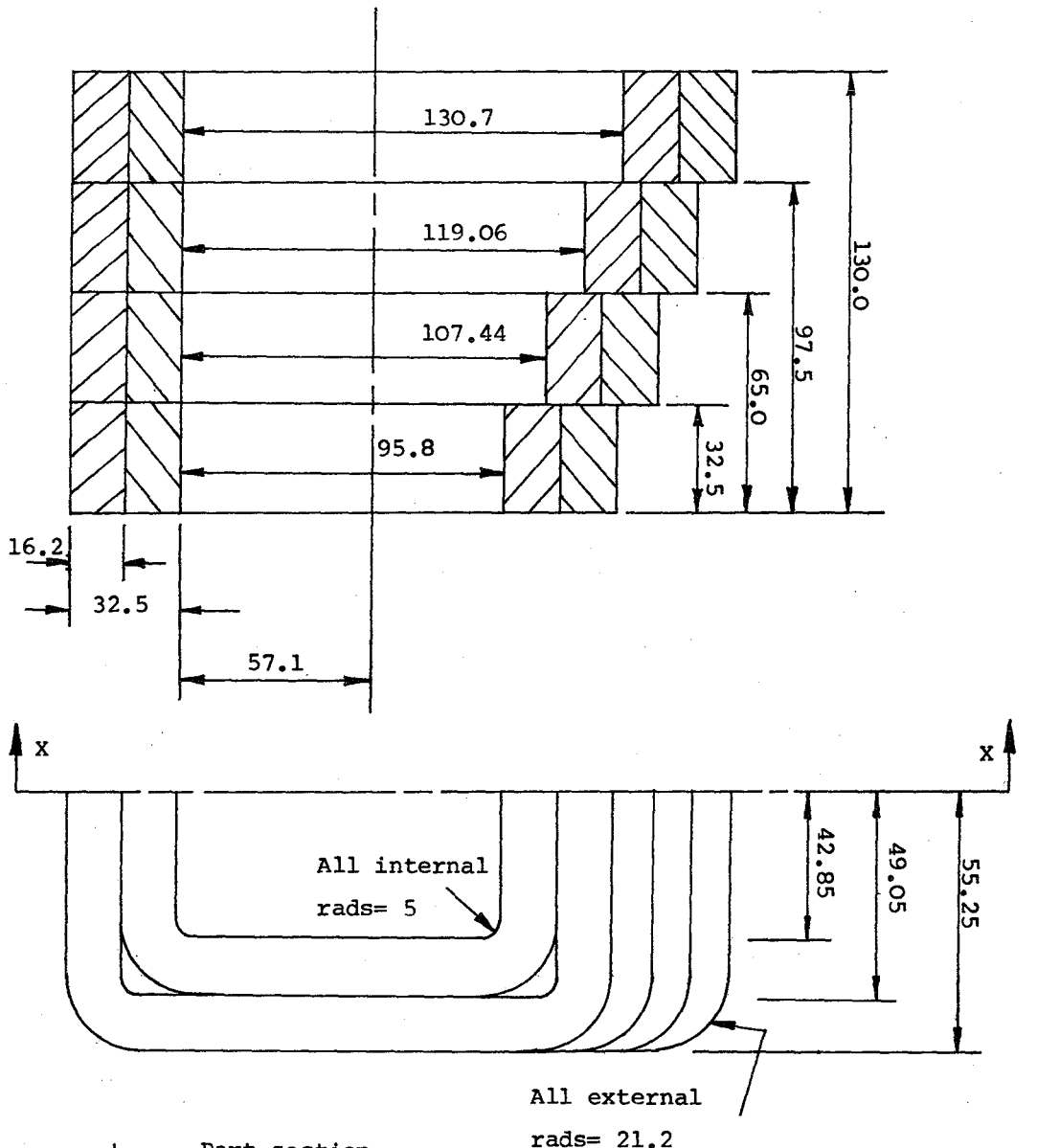

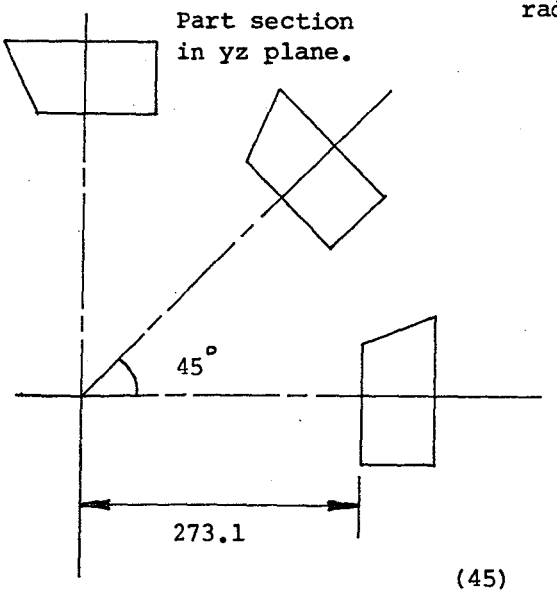

Fig.45 GFUN representation of Southampton E/Ms for torque computations.

Dims in cms.

GFUN calculations at 10 times true scale for convenience.
Scaled by Appendix I.
$J_{r,m}$=24.958 A/cm^2,
equivalent to 25A cable current.

GFUN data points are shown in Figures 46 and 47. Taking into consideration the extensive computational idealisations and various possible sources of experimental error, the agreement is considered to be excellent. The apparent discrepancies may, in fact, be unrepresentatively small (see Section 4.3), being less than the estimated experimental error alone. It is concluded that major systematic errors in the predictions of GFUN at low or moderate field levels are unlikely.

4.3. An assessment of likely accuracies of GFUN results

Considering previous results with GFUN (5, 6, 7, 8) regarding prediction of magnetization levels, the agreement between the GFUN torque integration scheme and an alternative method applied to a representative low field case (Section 4.1) and the performance of GFUN in predicting torque for the experimental system (Section 4.2), it is thought that the error magnitude in any GFUN prediction for the baseline or similar geometries at low applied field levels should not exceed 10%. Typical error may be significantly less than this figure, perhaps 5%. The error will tend to be mostly systematic in nature, available data showing very low random content. This implies that trends in performance should be reliably identified provided fairly consistant formulations of the problem (for instance element distributions) are used. This was in fact done. The effects of geometrical and other idealisations are not included in the above figures. It being anticipated that increased inaccuracy may occur with rising applied field levels and a predominantly saturated core it would seem appropriate to increase the figure for peak anticipated error to perhaps 20% for intermediate applied field levels (arbitrarily $2000 < J_{r,m} < 10000 A/cm^2$). At still higher applied field levels the predictions became progressively less relevant to immediate requirements (9) since the torques predicted are high and the peak E/M fields required to achieve those torques are outside the limits of existing technology (Section 5.2). The high applied field results ($J_{r,m} > 10000$ A/cm^2) should therefore, perhaps, be regarded for the time being as merely speculative and requiring further verification, such as testing of the GFUN torque integration scheme at high field levels.

Significant departures from the baseline core geometry (sweep, etc) are acheived only by utilising iron element distributions that are undesirably sparse. A version of GFUN exists (using the subprogram GETM 400) that can deal with up to 400 independant iron elements, rather than the 100 in the standard batch program, which could tackle most cases herein with nearly ideal element

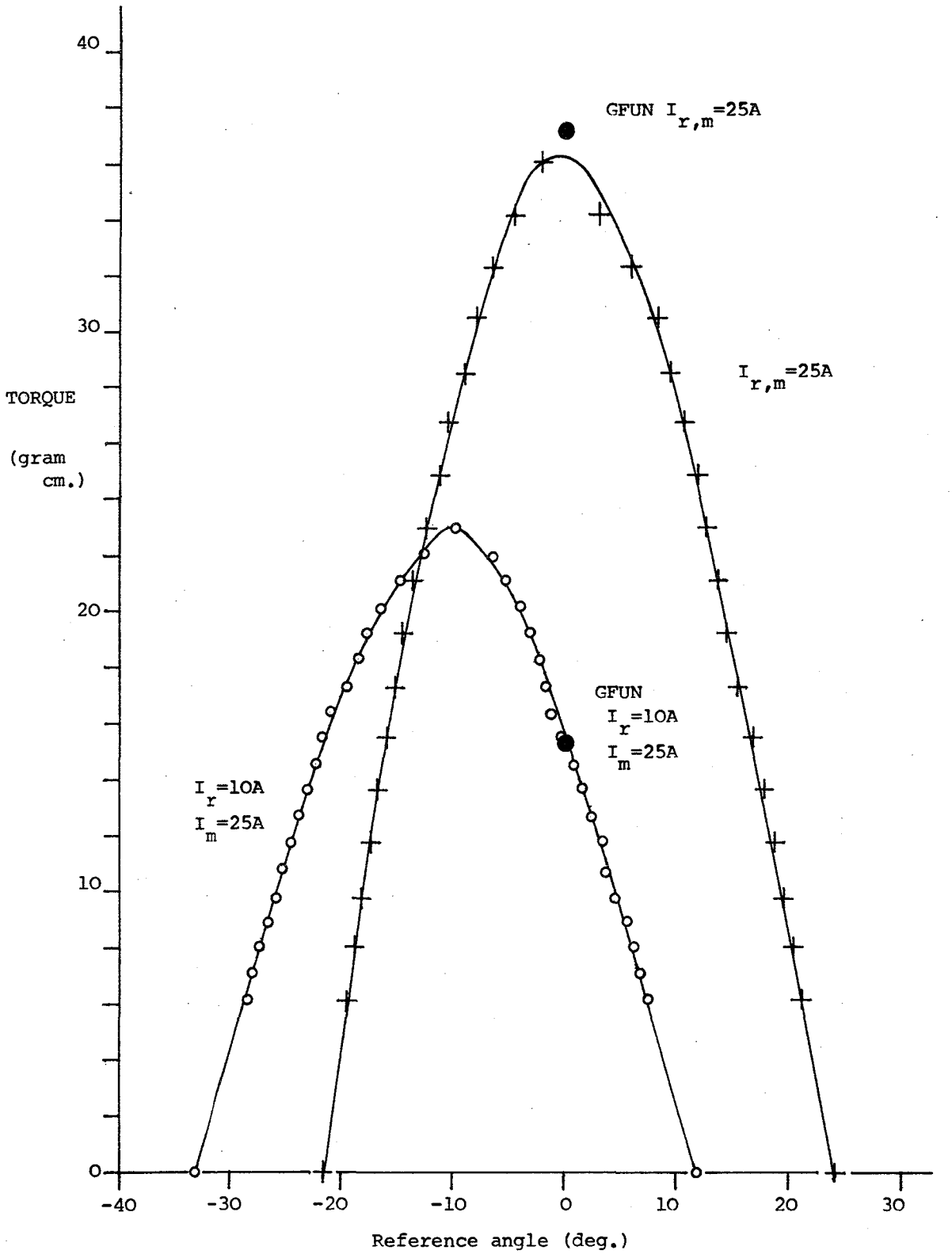

Fig.46 Comparison of GFUN data and selected experimental data for experimental 8 E/M SIM system.

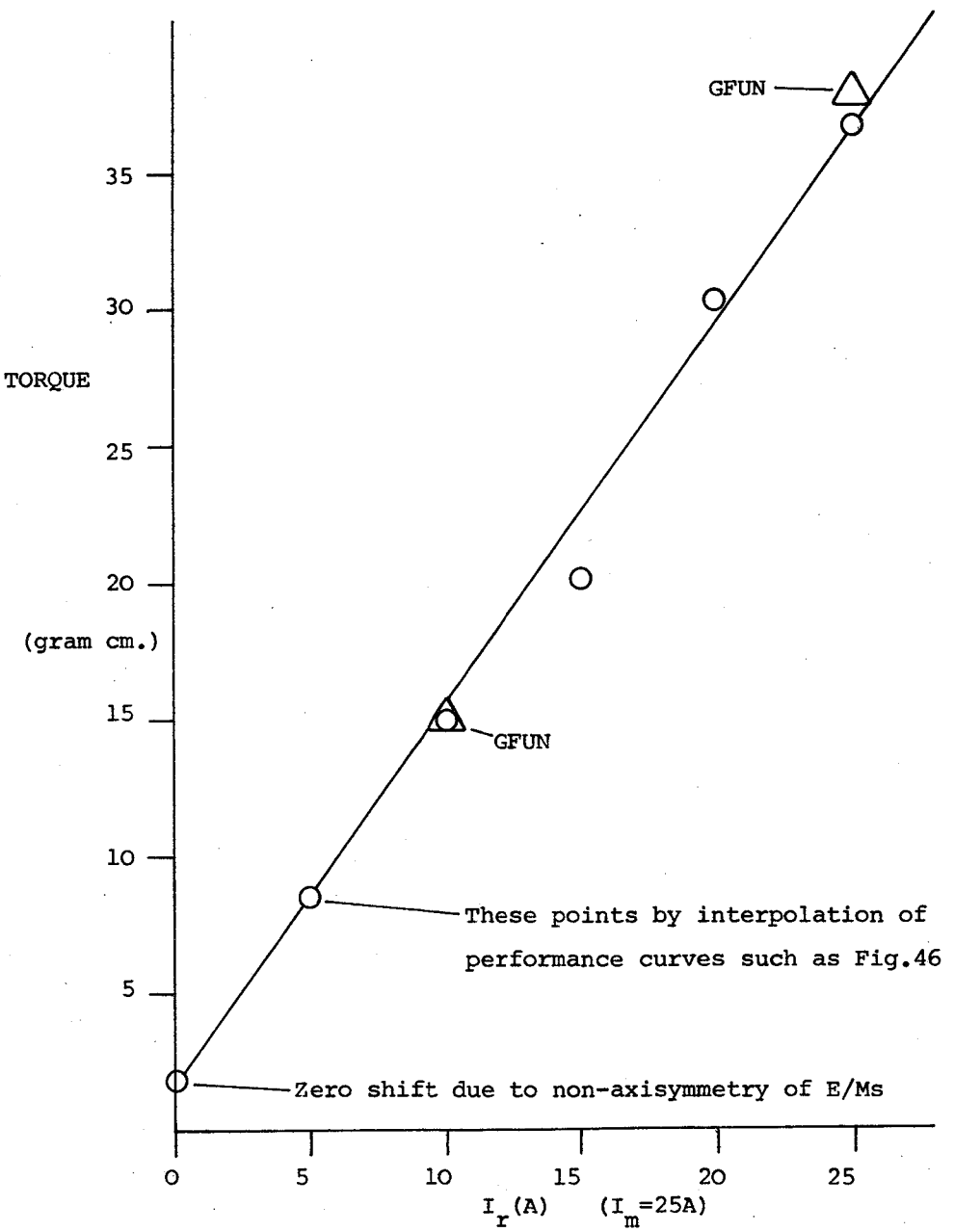

Fig.47 Comparison of measured (interpolated) and predicted (GFUN) roll torque for experimental 8 E/M SIM system

distributions. This facility did not become available during the period of this study and anyhow would require much greater CPU time for a solution, CPU time for solving the magnetizations being limited and varying approximately as the square of the number of iron elements. Thus, cases such as those involving core sweepback, the effect of axial fields and the F-16 cores, are subject to increased uncertainty.

Estimates of the likely peak error magnitudes in these cases are principally based on judgement but realistic estimates are thought to be:

Case	Peak anticipated error	Comments
Sweepback < 20°		Standard Integration volume.
low fields	20%	No useable symmetry.
Sweepback > 20°		
low fields	25%	Increased integration volume necessary
high fields positive Axial	30%	
high fields negative Axial	40%	Poor convergence of solutions
Axial field with fuselage		
low fields	20%	Large integration volume
high fields	30%	No useable symmetry.
F-16 low fields	40%	Undesirably sparse element
high fields	60%	distribution.

The principal idealisation inherent in all cases herein is the representation of wing chordwise cross sections (airfoil sections) as rectangles, since it has not (Section 2.2.) been thought that slab cores buried inside non-magnetic aerodynamic envelopes would be used in practice. In order that the existing GFUN predictions be applicable to MSBS cases with true airfoil sections some appraisal of the effects of this idealisation is necessary. However, it is not obvious on what basis, apart from cross sectional area, GFUN data can be matched to true sections. In the computed F-16 cases the moment of volume about the centroid of area was chosen arbitrarily to generate a GFUN representation. The thickness to chord ratio, defined conventionally, could also be used, leading to generally similar results with classical streamline wing sections. Typical comparison between a GFUN section and a true section is shown in Figure 48.

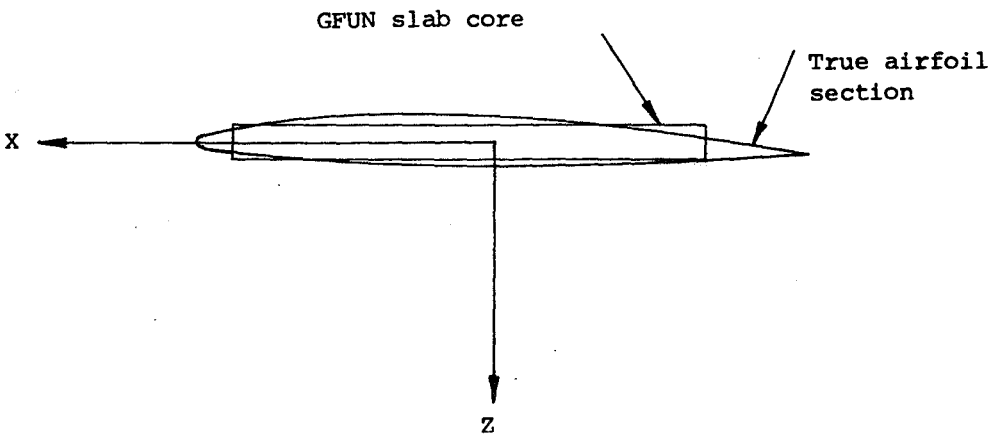

Fig.48 Comparison of GFUN and true core cross sections.

Since the spanwise slenderness is scarcely affected, it is expected that the mean spanwise magnetizations should be near identical in both cases, though the detail distributions must be different. The chordwise and through wing slenderness will be affected by the change of section, though the precise value of through wing slenderness is not thought to be critical at low or moderate fields. The (increased) chordwise slenderness with the true section will lead to somewhat greater sensitivity to axial fields, the amount by which the effects of the axial field are amplified being perhaps in the range 0 - 50%.

5. DISCUSSION AND CONCLUSIONS

5.1 Further use of GFUN in SIM computations

GFUN's creators could not have envisaged that it would see use in this type of problem. Because of this several detail features are inconvenient for SIM computations. Some of these, such as the lack of a proven torque integration scheme, have been partially rectified (by Simkin at Rutherford Laboratory) during the course of this study, but some remain. Examples are the inability to exploit all the symmetry existing in all problems, the lack of a torque integration scheme with the high element number version of GFUN, and the doubts concerning torque predictions at high applied field levels. It is beleived that these difficulties can be overcome relatively easily by further improvements/expansions to the program

code. If this were done it seems likely that GFUN could provide torque (and force) predictions to a much higher level of accuracy then those estimated for the results herein. Definition of E/M and model core requirements for specific performance demands (all degrees of freedom) for specific LMSBSs should then be possible, to adequate accuracy for preliminary and intermediate LMSBS design and cost studies. It is difficult to imagine GFUN or similar programs becoming sufficiently accurate for precise prediction of performance (say better than 1% accuracy) in all cases of interest due principally to the geometrical idealisations required in the formulations of the problem, though this level of accuracy should be attainable for certain simple cases. Empirical calibration of practical systems would therefore appear mandatory. Universally high accuracy may, however, be considered unnecessary, for instance where significant over-capacity is incorporated in LMSBS E/Ms.

5.2. Application of the SIM system to LMSBS

Even taking account of the relatively large errors considered likely to exist in the computed results it is clear that the apparent torque capability of the SIM system considerably exceeds those predicted **heretofore** for other rolling moment generating systems. Subject to the provision of adequately powerful E/Ms the SIM scheme must be considered a viable contender for LMSBS application. The matter of E/M design must be tackled separately, but data is included (Figure 49) showing the baseline magnetizing field at 1000 A/cm^2. The baseline through-wing field is similar but indexed by 45°. Examining the available data it is difficult to imagine the specified E/Ms being operated above, perhaps, 3000 A/cm^2, with existing technology superconductors, whence the peak field within their bores becomes approximately 6.6 T. That value of field will not be increased by geometrical adjustments, only by improvements in superconducting E/M technology. Whilst certain optimisations of E/M geometry remains possible, it is seen that a fundamental limit to the available torque from a particular SIM system exists.

Where peak performance is required is is easily seen that the E/Ms should be located as close to the model as possible (Figure 50).

This study has indicated that at least with respect to available roll torque, the SIM system is viable for application to LMSBSs.

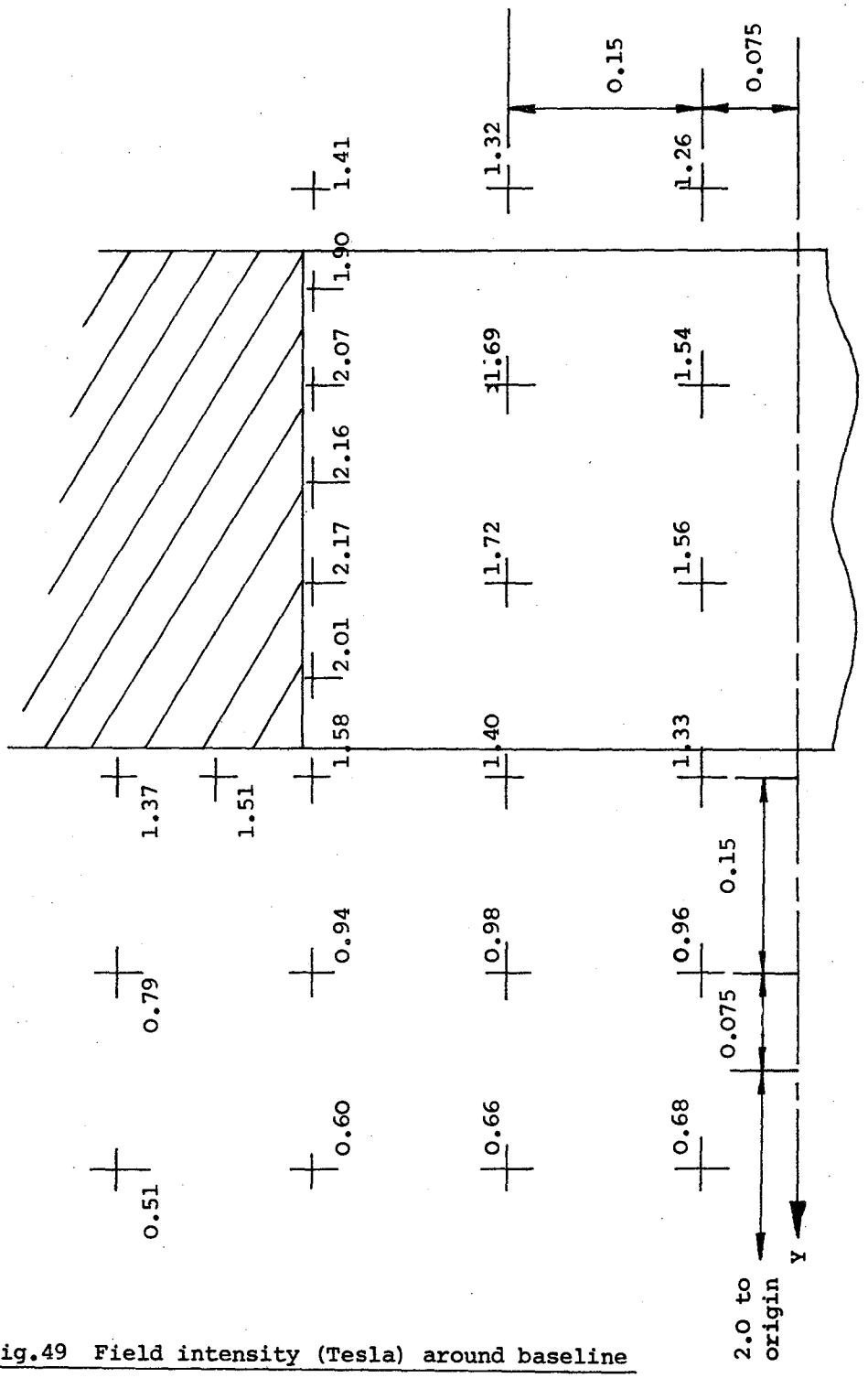

Fig.49 Field intensity (Tesla) around baseline magnetizing field E/Ms. $J_r=0$ $J_m=1000$ A/cm^2

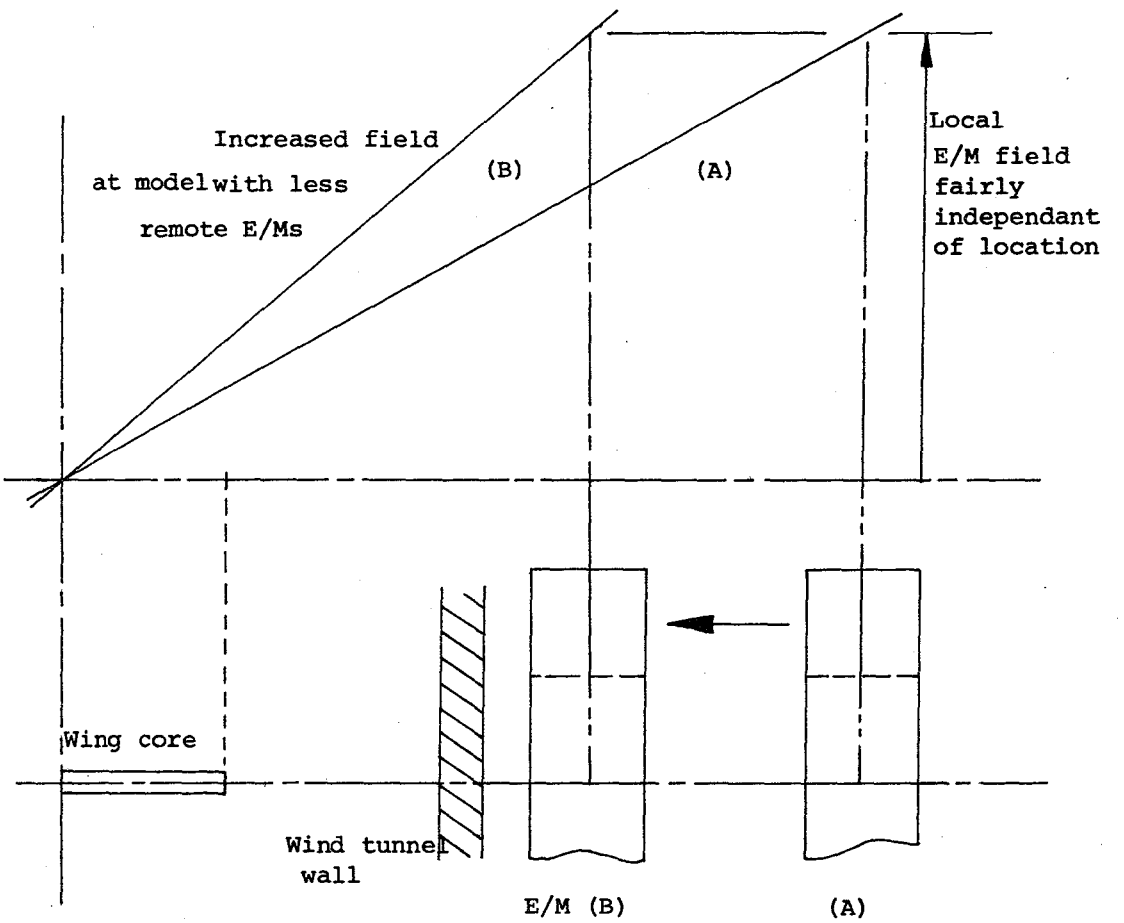

Fig.50 Improvement in E/M effectiveness with closer packing to wind tunnel wall.

5.3. Further aspects of SIM performance

The matter of cross couplings between roll and other degrees of freedom due to the presence of the spanwise magnetizations, or the (applied) wing core magnetizing or through wing fields, has not been addressed here. Some treatment will be attempted in Reference 13. It happens that with unswept wings (predominantly spanwise magnetizations) there exists only one primary interaction, that is coupling into yaw from a sideforce demand. It is not thought that this presents any serious difficulty since the magnitude of aerodynamic forces and moments in the lateral plane are generally smaller than in the vertical plane, whereas the magnetic force and moment capability due to the axial (fuselage) magnetization will often be approximately equal in the two planes.

General cases, such as the F-16 geometry, will be expected to exhibit complex couplings, mostly second order in magnitude, due to the presence of axial magnetization components in the models wings and the lack of fore-and-aft symmetry of the spanwise magnetizations.

REFERENCES

1. Haldeman, C.W., Kramer, R.A., Way, P. (Massachusetts Institute of Technology) Developments at MIT related to magnetic model suspension and balance systems for large scale facilities. Paper No. 9. First International Symposium on Cryogenic Wind Tunnels. Southampton University, Department of Aeronautics and Astronautics, April 1979

2. Britcher, C.P., Fortescue, P.W., Allcock, G.A., Goodyer, M.J. Preliminary investigations of design philosophies and features applicable to large magnetic suspension and balance systems. NASA CR-162433 November 1979

3. Chari, M.V.K., Silvester, P.P. (Eds). Finite elements in electrical and magnetic field problems. Wiley 1980

4. Binns, K.J., Lawrenson, P.J. Analysis and computation of electrical and magnetic fields. Pergamon 1963

5. Newman, M.J., Trowbridge, C.W., Turner, L.R. GFUN: An interactive program as an aid to magnet design. 4th International Conference on Magnet Technology. Brookhaven, September 1972

6. Armstong, A.G.A.M., Collie, C.J., Diserens, N.J., Newman, M.J., Simkin, J., Trowbridge, C.W. New developments in the magnet design program GFUN. 5th International Conference on Magnet Technology. Frascati, Rome, 1975. Also Rutherford Laboratory RL-75-066, March 1975

7. Trowbridge, C.W. Applications of integral equation methods for the numerical solution of magnetostatic and eddy current problems. Rutherford Laboratory RL-76-071, June 1976

8. Armstrong, A.G.A.M., Collie, C.J., Diserens, N.J., Newman, M.J., Simkin, J., Trowbridge, C.W. GFUN 3D users guide. Rutherford Laboratory RL-76-029, November 1976, revised August 1979

9. General Electric Company. Design concepts and cost studies for magnetic suspension and balance systems; final report. Document No. 81LSP47251, March 1981

10. Bozorth, R.M. Ferromagnetism. Van Nostrand 1951

11. Boll, R. (Ed) Soft magnetic materials (the Vacuumschmelze Handbook) Vacuumschmelze GmbH. Hanau. Heyden 1979

12. Goodyer, M.J. The magnetic suspension of wind tunnel models. Southampton University, Department of Aeronautics and Astronautics, April 1968

ACKNOWLEDGEMENTS

The work reported herein forms part of the program of research undertaken under NASA Grant NSG-7523. The Principal Investigator is Dr. M.J. Goodyer and the NASA Langley Technical Monitor is Richmond P. Boyden.

The computer facilities and support services essential for the SIM computations were provided by the British Science Research Council under Grant No. GR/B/3691.5. Special thanks must go to Mr. John Simkin of the Rutherford Laboratory for his effort and co-operation in adapting GFUN for this work.

APPENDIX 1

Scaling of results to other physical sizes

Exact equivalence of results at different physical scales is obtained if the applied field is made equal to all corresponding points in each scale. This is **achieved** with consistent geometry if the E/M current density is varied as the factor:

$$J \propto \frac{1}{\text{Scale}}$$

Since the field around and the magnetization within the SIM cores are unaltered, torque for any particular case will vary as:

$$\text{Torque} \propto \text{Scale}$$

Technological limitations on E/M performance are functions of scale, in particular the useable current density falls with increasing scale, but the trends are not continuous, apparently involving enforced abandonment of particular conductor technologies at specific limiting scales. Further treatment of these effects cannot be attempted here.

1. Report No.	2. Government Accession No.	3. Recipient's Catalog No.
NASA CR-165888		

4. Title and Subtitle	5. Report Date
AN ASSESSMENT OF THE PERFORMANCE OF THE SPANWISE IRON MAGNET ROLLING MOMENT GENERATING SYSTEM FOR MAGNETIC SUSPENSION AND BALANCE SYSTEMS, USING THE FINITE ELEMENT COMPUTER PROGRAM "GFUN"	MARCH 1982
	6. Performing Organization Code
7. Author(s) C. P. Britcher	8. Performing Organization Report No.
	10. Work Unit No.
9. Performing Organization Name and Address The University of Southampton Department of Aeronautics and Astronautics Southampton SO9 5NH, ENGLAND	11. Contract or Grant No. NSG-7523
	13. Type of Report and Period Covered 11-1-80 Contractor Report 11-1-81
12. Sponsoring Agency Name and Address National Aeronautics and Space Administration Washington, DC 20546	14. Sponsoring Agency Code 505-31-53-06

15. Supplementary Notes

Principal Investigator was Dr. M. J. Goodyer

16. Abstract

Development of a powerful method of magnetic roll torque generation is essential before construction of a Large Magnetic Suspension and Balance System (LMSBS) can be undertaken. This report presents some preliminary computed data concerning a relatively new D.C. scheme, referred to as the Spanwise Iron Magnet scheme. Computations have been made using the finite element computer program 'GFUN' and indicate that adequate torque is available for at least a first generation LMSBS. Torque capability appears limited principally by current electromagnet technology.

17. Key Words (Suggested by Author(s))	18. Distribution Statement
Magnetic suspension Rolling moment GFUN computer program	Unclassified - Unlimited Star Category - 09

19. Security Classif. (of this report)	20. Security Classif. (of this page)	21. No. of Pages	22. Price*
Unclassified	Unclassified	60	A04

For sale by the National Technical Information Service, Springfield, Virginia 22161

End of Document